AD-A035 697 TEXAS UNIV AT AUSTIN APPLIED RESEARCH LABS F/G 20/1
ANALYTICAL TECHNIQUES FOR DETERMINING SUBBOTTOM VELOCITY PROFIL--ETC(U)
DEC 76 S R RUTHERFORD N00039-76-C-0081
UNCLASSIFIED ARL-TR-76-58 NL

1 OF 2
AD A035697

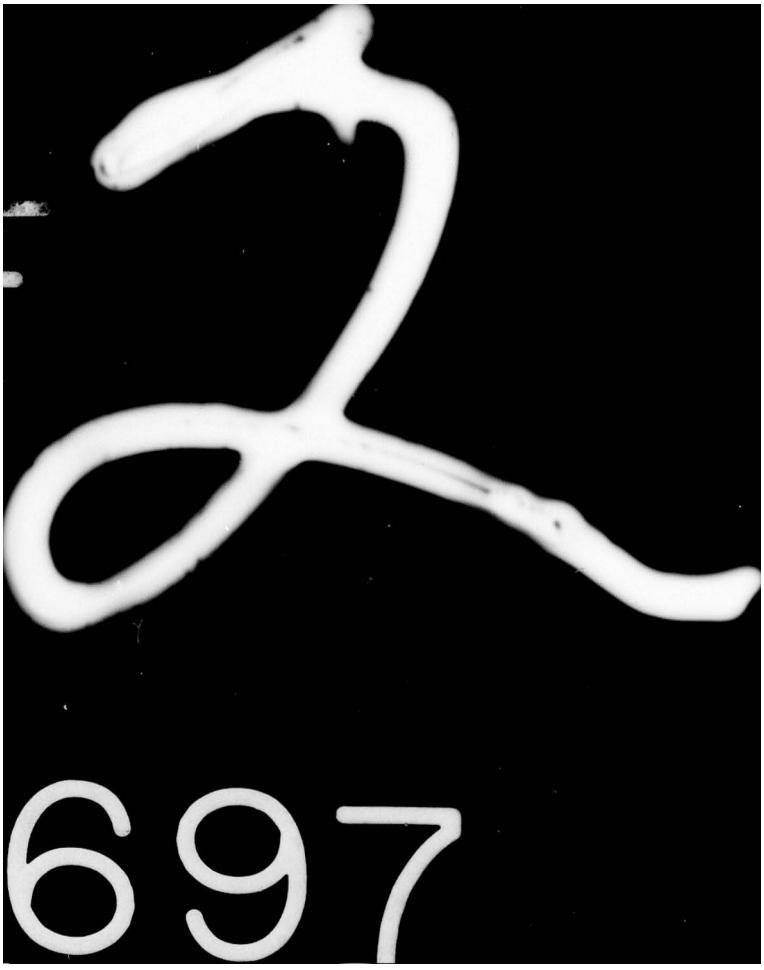
697

(12)

FG.

APPLIED RESEARCH LABORATORIES

THE UNIVERSITY OF TEXAS AT AUSTIN

ARL-TR-76-58
21 December 1976

Copy No. 69

ANALYTICAL TECHNIQUES FOR DETERMINING SUBBOTTOM VELOCITY PROFILES IN UNCONSOLIDATED SEDIMENTS

Steven R. Rutherford

NAVAL ELECTRONIC SYSTEMS COMMAND
Contract N00039-76-C-0081

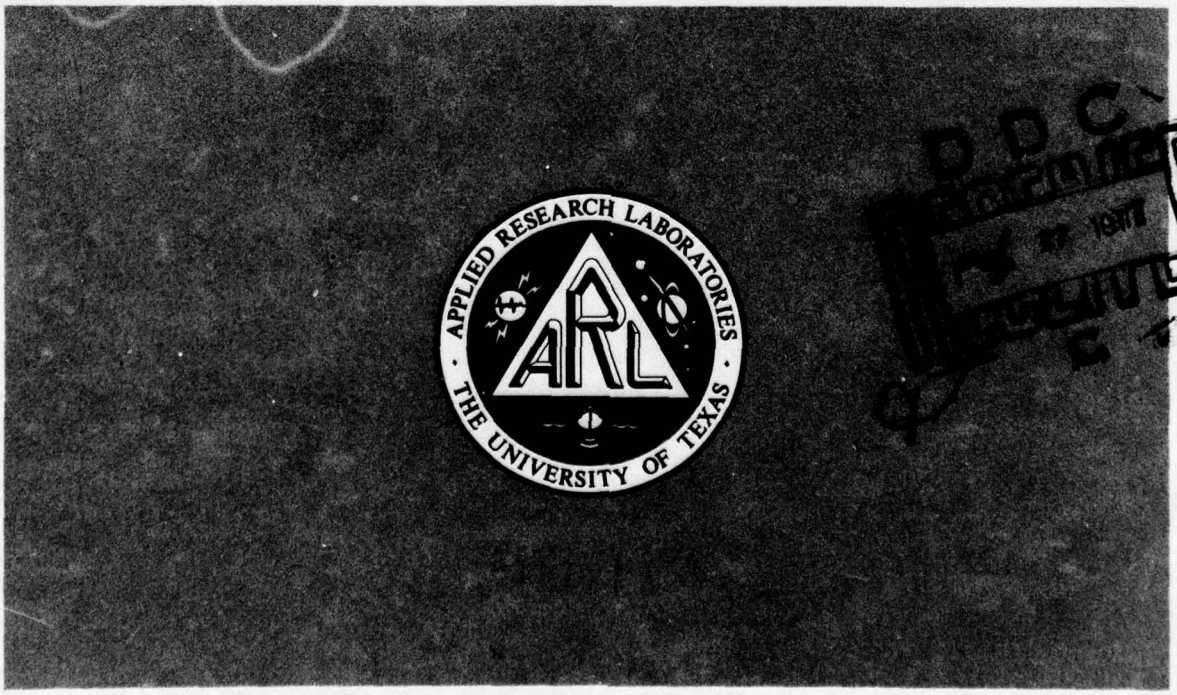

SECURITY CLASSIFICATION OF THIS PAGE (When Data Entered)

REPORT DOCUMENTATION PAGE

READ INSTRUCTIONS BEFORE COMPLETING FORM

1. REPORT NUMBER: ARL-TR-76-58	2. GOVT ACCESSION NO.
3. RECIPIENT'S CATALOG NUMBER	
4. TITLE (and Subtitle): ANALYTICAL TECHNIQUES FOR DETERMINING SUBBOTTOM VELOCITY PROFILES IN UNCONSOLIDATED SEDIMENTS.	5. TYPE OF REPORT & PERIOD COVERED: technical report.
	6. PERFORMING ORG. REPORT NUMBER
7. AUTHOR(s): Steven R. Rutherford	8. CONTRACT OR GRANT NUMBER(s): N00039-76-C-0081
9. PERFORMING ORGANIZATION NAME AND ADDRESS: Applied Research Laboratories, The University of Texas at Austin, Austin Texas 78712	10. PROGRAM ELEMENT, PROJECT, TASK AREA & WORK UNIT NUMBERS: —
11. CONTROLLING OFFICE NAME AND ADDRESS: Naval Electronic Systems Command, Department of the Navy, Washington, D. C. 20360	12. REPORT DATE: 21 December 1976
	13. NUMBER OF PAGES: 95
14. MONITORING AGENCY NAME & ADDRESS (if different from Controlling Office): — (12) 95p.	15. SECURITY CLASS. (of this report): UNCLASSIFIED
	15a. DECLASSIFICATION/DOWNGRADING SCHEDULE: —

16. DISTRIBUTION STATEMENT (of this Report)

Approved for public release; distribution unlimited.

17. DISTRIBUTION STATEMENT (of the abstract entered in Block 20, if different from Report)

—

18. SUPPLEMENTARY NOTES

—

19. KEY WORDS (Continue on reverse side if necessary and identify by block number)

travel time data analysis
reflected arrival methods
refracted arrival methods
interval velocities
sound speed gradients

20. ABSTRACT (Continue on reverse side if necessary and identify by block number)

This report describes and discusses some of the most common and widely used methods for analyzing travel time data to obtain the layer and velocity structures in marine subbottom sediments. Two methods for analyzing travel time data of arrivals reflected from subbottom layers to determine interval velocities and layer thicknesses are discussed and shown to give acceptable results when applied to a range of differing water-sediment thickness ratios. A method for analyzing interval velocities to yield sound speed as a function

DD FORM 1 JAN 73 1473 EDITION OF 1 NOV 65 IS OBSOLETE

UNCLASSIFIED

SECURITY CLASSIFICATION OF THIS PAGE (When Data Entered)

404 434

20. (cont'd)

of depth is presented and shown to be capable of accurately determining subbottom velocity profiles under restrictive conditions. Two methods which may be used in a single sediment layer configuration are also presented; both of these methods are based on the effects of sound energy which has refracted in the subbottom and are capable of determining the initial sound velocity and gradient in the single layer. (U)

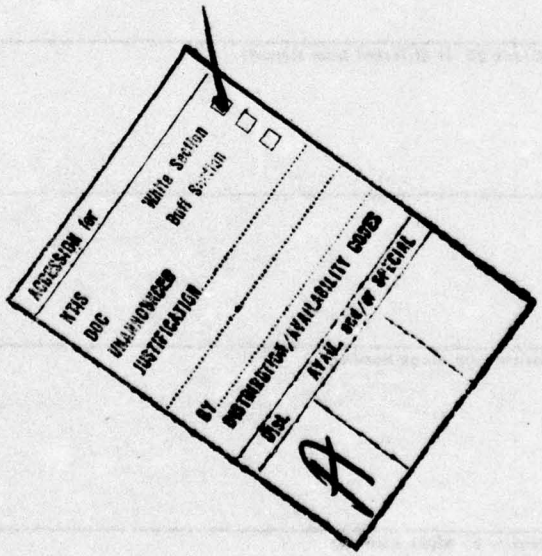

ARL-TR-76-58
21 December 1976

ANALYTICAL TECHNIQUES FOR DETERMINING SUBBOTTOM VELOCITY PROFILES IN UNCONSOLIDATED SEDIMENTS

Steven R. Rutherford

NAVAL ELECTRONIC SYSTEMS COMMAND
Contract N00039-76-C-0081

APPLIED RESEARCH LABORATORIES
THE UNIVERSITY OF TEXAS AT AUSTIN
AUSTIN, TEXAS 78712

ABSTRACT

This report describes and discusses some of the most common and widely used methods for analyzing travel time data to obtain the layer and velocity structures in marine subbottom sediments. Two methods for analyzing travel time data of arrivals reflected from subbottom layers to determine interval velocities and layer thicknesses are discussed and shown to give acceptable results when applied to a range of differing water-sediment thickness ratios. A method for analyzing interval velocities to yield sound speed as a function of depth is presented and shown to be capable of accurately determining subbottom velocity profiles under restrictive conditions. Two methods which may be used in a single sediment layer configuration are also presented; both of these methods are based on the effects of sound energy which has refracted in the subbottom and are capable of determining the initial sound velocity and gradient in the single layer.

ACKNOWLEDGEMENTS

The author of this report wishes to acknowledge the guidance and assistance given by the following people during the preparation of the report. First, the author acknowledges Dr. Aubrey L. Anderson of ARL/UT for his assistance in outlining the basic goals and purpose of this report and for his comments and suggestions as to the final form of the text. Second, Drs. Kenneth E. Hawker and Loyd D. Hampton of ARL/UT are acknowledged for their comments and suggestions concerning the form of this report. The author also acknowledges Terry L. Foreman of ARL/UT for his assistance in familiarizing the author with his ARL/UT ray tracing programs PROBE and RANGER and for the "spline-fit" program that he coded for use in calculating the velocity and gradient functions of Chapter III. Jan Draeger of Bundersant für Wehrtechnik und Beschaffung in the Federal Republic of Germany is acknowledged for his notes and his ideas concerning sound speed gradient information from the ray parameter method.

TABLE OF CONTENTS

TABLE OF CONTENTS (Cont'd)

I. INTRODUCTION

The purpose of this report is to discuss and to describe different analytical methods for determining velocity profiles in unconsolidated sediments from experimental data. This report is by no means exhaustive; its intent has been to assemble in one place those methods which would be most useful to underwater sound propagation modelers and best suited to the types of data that they will usually have access to.

There are different ways of obtaining information about the velocity structure of the subbottom. In shallow water, divers with probes can take samples of the upper few meters of sediment for later lab analysis. A somewhat deeper probing of the sediment structure is possible with sediment coring apparatus deployed from a research vessel. The cores thus obtained may be analyzed in the laboratory or the velocity profile of the sediment may be measured in situ with a device such as the ARL Compressional Wave Profilometer,[1] which can be attached to a corer. These direct methods are limited by the depths that a corer can probe, or roughly 30 meters. The only other direct methods involve the analysis, either in situ or laboratory, of drilling cores. This method, though very useful in many acoustic studies, relies on well cores which are often widely spaced and must be supplemented with other methods.

The methods addressed in this report are indirect, acoustical techniques, which more often than not provide the only way of estimating the velocity structures of the unconsolidated sediments to the depths required by underwater propagation modelers. These indirect methods will be concerned only with the unconsolidated sediments though some of the methods can be and are used in seismic profiling. Seismological methods such as those involving lateral and shear waves are not discussed in this report.

This report is primarily intended to serve the needs of those working in the field of underwater sound propagation modeling who have little knowledge of the techniques for extracting subbottom velocity information which is necessary input for their models. An example of such a usage is the ARL/UT propagation studies using BOTLOSS,[2] a program that requires the sediment velocity profile as input. BOTLOSS calculates a plane wave reflection coefficient for a multilayered sediment structure overlying a solid substrate and is used in a ray theory propagation model and in various sensitivity studies. It is applications such as these that the report addresses.

The different analysis techniques discussed in this report may be divided into three categories which are treated in Chapters II, III, and IV.

A. Reflected Arrival Methods

Chapter II treats the reflected arrival methods, which are of two types, the $T^2(X)$ methods and the ray parameter methods. There are three $T^2(X)$ methods: the reduced time-reduced distance method, the small range method,[3,4] and Dürbaum's[5] Method.

All of the $T^2(X)$ methods are derived under the assumption that the water and sediment layers in question are isovelocity. This assumption has the effect of restricting the $T^2(X)$ methods to small water layer-sediment layer thickness ratios (less than 15:1). Each of these methods, though they approach the solutions in different ways, relies on the fact that the relation between the travel time of a ray reflecting in a single isovelocity layer and the range attained while traveling through that layer is a hyperbolic one ($T^2=A+BX^2$).

The $T^2(X)$ methods develop techniques for determining the velocity of sound in a layer and the thickness of the layer by analyzing travel

time curves of ray paths that have reflected off the bottom of the layer in question. (A travel time curve is simply a curve depicting the relation between the range and the travel time required to attain that range of rays traveling between source and receiver positions at fixed depths.) When the layer in question is underlying other layers it is necessary to subtract the effect of the overlying layers so that the hyperbolic relation between T and X in a single layer may be used to yield the layer velocity.

In the text of Chapter II the reduced time, reduced distance method and the small range method are illustrated with examples. Both of these methods are used to find the layer velocity in a 200 m thick sediment layer underlying a 500 m thick water layer (thickness ratio 2.5:1). The reduced time, reduced distance method determined a layer velocity of 1539 m/sec and the small range method yielded 1575 m/sec. The standard value calculated from the results of Appendix A was 1561 m/sec which yielded percent differences of 1.4 and 0.89, respectively.

The ray parameter method,[6] which is the second of the reflected arrival methods, is fundamentally different from the $T^2(X)$ methods, though it too analyzes travel time data of ray paths which have reflected off subbottom reflecting horizons. The ray parameter method is unique in that water or sediment layers overlying the layer to be analyzed are irrelevant to the solution so that the velocity structure above the layer does not need to be dealt with. Therefore the ray parameter methods can be used for much larger water layer-sediment layer thickness ratios (up to 500:1).

The ray parameter method is so named because it compares the ray paths of the same ray parameter which have reflected off the top and bottom of the layer in question. The ray parameter is defined by $p=\cos\theta(z)/c(z)$ and is calculated from travel time data by evaluating the derivative of a travel time curve, i.e., $p=dT/dx$. Two different

types of ray parameter methods are discussed in this report, the 'normal method' and the 'thin layer approximation'.[6] Both methods calculate the sound velocity and thickness of a particular layer by matching the derivatives of travel-time curves. The thin layer approximation incorporates a graphical technique which alleviates instabilities associated with thin layers.

An example of the thin layer approximation is considered in Chapter II. This method is applied to a single sediment layer 50 m thick underlying a 5000 m water layer (thickness ratio 100:1). In this example the thin layer approximation yielded a layer velocity of 1549 m/sec, which compares favorably with the value calculated from the results of Appendix A (1565 m/sec).

B. The V(t) Method

Chapter III discusses a method whereby velocity measurements obtained by reflected arrival methods may be analyzed to construct a velocity profile throughout the sediment layers. As stated earlier, the reflected arrival methods determine a layer velocity under the isovelocity assumption, a condition which is rarely met in the physical world. For this reason, the velocities calculated by the methods of Chapter II are interpreted as 'interval velocities' which are assumed to be the time averaged sound velocity in a particular layer or interval.

The V(t)[7,8] method is a method for analyzing interval velocities to obtain velocity gradients and layer thicknesses throughout the sediment layer structure. The method is based on a velocity function which is formed by fitting the layer or interval velocities to a polynomial in t, the one-way vertical travel time to the time midpoint of the various layers on the sediment structure. Once the velocity function is known, a gradient function and a depth function which specify the gradient and depth as a function of t may easily be determined.

The effects of velocity discontinuities across layer boundaries and uncertainties in the interval velocities are shown to be significant in some situations and tend to have an adverse effect on the confidence one has in the results. In particular, velocity discontinuities yielded layer gradients in error by an average of 30% as opposed to average differences of 1% when velocity discontinuities were absent.

C. The Refracted Arrival Methods

Chapter IV discusses two refracted arrival methods: Dicus' Method[9] and Hanna's method.[10] These methods differ from the reflected arrival methods in that the effects of shallow refracted arrivals instead of reflected arrivals are analyzed; also, these methods assume a gradient exists in the sediment layer. It is expected that both of these methods would most successfully be applied to thick, single sediment layers. The term 'refracted arrival' should not be confused with arrivals resulting from lateral or interface waves; it means those arrivals that are returned from the sediment layer by virtue of a turning point arising because of a velocity gradient.

Dicus' method is a graphical method which deals with the time differences of the refracted arrivals and the arrivals that attain the same receiver position via one bottom reflection. The method is derived assuming a pseudolinear sediment velocity profile and yields the gradient at the top of the sediment layer and the ratio of velocities at the water-sediment interface as output.

As an example, Dicus' method is applied to a single sediment layer with a constant gradient of 1 sec^{-1} having a velocity ratio at the water sediment interface of 1.0333. Dicus' method calculated a velocity ratio of 1.0358 and a gradient at the top of the layer of 0.99 sec^{-1}, which correspond to differences of 0.24% and 1% respectively.

Finally, a completely different method due to Hanna is considered. This technique yields the same output as Dicus' method by an analysis of the nulls in propagation loss curves which arise because of the interference produced by refracted arrivals. This method also models the sediment with a pseudolinear velocity profile.

II. REFLECTED ARRIVAL METHODS

This chapter discusses the most common and widely used methods of interval velocity analysis, the reflected arrival methods. The term reflected arrival methods is used because these methods deal with arrivals that have reflected off the bottom or subbottom layers, as opposed to methods dealing with arrivals that have refracted through the bottom.

Both of the methods to be discussed analyze travel time curves from a layered sound medium. A travel time curve can be constructed for each reflecting surface, and this travel time curve is simply the relationship between the horizontal range and the time required for a sound ray to attain that range via one reflection from the layer in question. Though both methods approach the problem in different ways, each extracts the velocity of sound in the layers and the thicknesses of the layers from travel time data.

The travel time data to which these methods will be applied are all obtained in a similar manner. In general, a ship deploying TNT charges or towing an acoustic source travels away from a configuration of hydrophones which are either physically connected to another ship or are attached to sonobouys. As the source ship travels away from the hydrophones, the charges or acoustic sources are activated at given intervals. Timing circuitry is used to determine the travel times of the arrivals received by the hydrophones, and this travel time is used in conjunction with the horizontal distances between source and receiver to construct a travel time curve (i.e., travel time versus horizontal range).

When charges are used as the acoustic source, the travel time data will be of a discrete nature. When sources such as towed sparkers are used, more continuous travel time curves will be generated. This

continuous data is usually presented in the form of analog paper strip charts that are generated on board ship. These strip charts give a relatively continuous depiction of the travel times of the various arrivals versus horizontal distance, or ship cruise time.

To obtain usable mathematical expressions the derivations discussed in this chapter are based on an assumption of isovelocity layers. Unfortunately, isovelocity is rarely the situation in the physical world. Most often this method is used to find the sound speeds in the subbottom sediment layers of a configuration in which the top layer is a relatively thick water layer and the underlying layers are thinner sediment layers known to have rather significant sound speed gradients. The sediment layer sound speeds will be interpreted as 'layer velocities' or 'interval velocities'. These are the time averaged sound speeds in the layers and are defined by (see Appendix A),

$$C_{int}^{\ 2} = \frac{1}{\Delta T} \int_{o}^{\Delta T} C^2(T)dT \quad ,$$

where ΔT is the two-way vertical reflection time for the layer and $C(T)$ is the sound speed as a function of time for the layer.

A. The $T^2(X)$ Method

The $T^2(X)$ method is one in which the square of the arrival times of a reflected arrival, T, are fit to a polynomial in X, the horizontal range. Usually the polynomial in X is quadratic but more advanced analysis includes terms to the fourth power.

The $T^2(X)$ method is based on analysis done by Green[11] in 1938. If one considers the ray path through an isovelocity layer as depicted

in Fig. II.1, then it is possible to write the following equation for the ray path length,

$$S^2 = X^2 + (2H)^2 \quad . \qquad \text{II.1}$$

Since the layer is assumed to be isovelocity, the above equation may be divided by the square of the water velocity, C_1, to yield

$$T^2(X) = T^2(0) + \frac{1}{C_1^2} X^2 \quad . \qquad \text{II.2}$$

$T^2(X)$ is the reflection travel time at range X and $T^2(0)$ is the vertical reflection time at the origin. From the form of Eq. II.2 it is obvious that the relation between $T^2(X)$ and X^2 is a linear one with the slope being C_1^{-2} and the intercept being $T^2(0)$. This relationship is exact for an isovelocity single layer configuration. Green first used Eq. II.2 to calculate sound speeds by plotting $T^2(X)$ and X^2 values obtained from seismic measurements and measuring the slope of the resulting graph. When the configuration is changed to a more realistic one in which added layers with differing velocities are considered, the linear relation between $T^2(X)$ and X^2 is destroyed.

To illustrate the $T^2(X)$ method and its different versions, consider the configuration of two isovelocity layers depicted in Fig. II.2. The ray path labeled R_{11} can be analyzed using Green's method since its path is wholly within one layer; the path labeled R_{12} cannot since it traverses two layers. To handle this latter situation, Dix (1955) modified Green's method.

1. <u>The Reduced Time, Reduced Distance Method</u>

To calculate the velocity in layer 2, information from paths like R_{12} must be analyzed. As mentioned earlier, for paths like these

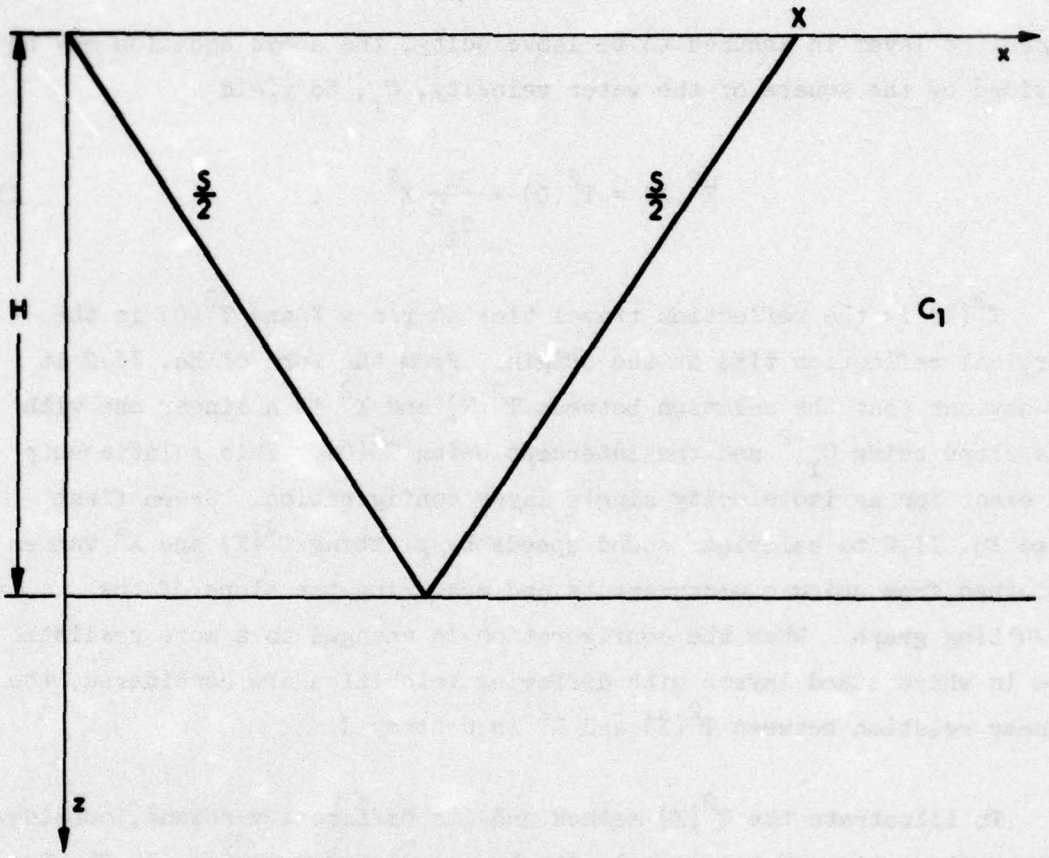

FIGURE II.1
REFLECTION RAY PATH GEOMETRY FOR A FLAT LYING LAYER OF THICKNESS H AND CONSTANT SOUND VELOCITY, C_1

ARL - UT
AS-76-1170
SRR - DR
11 - 2 - 76

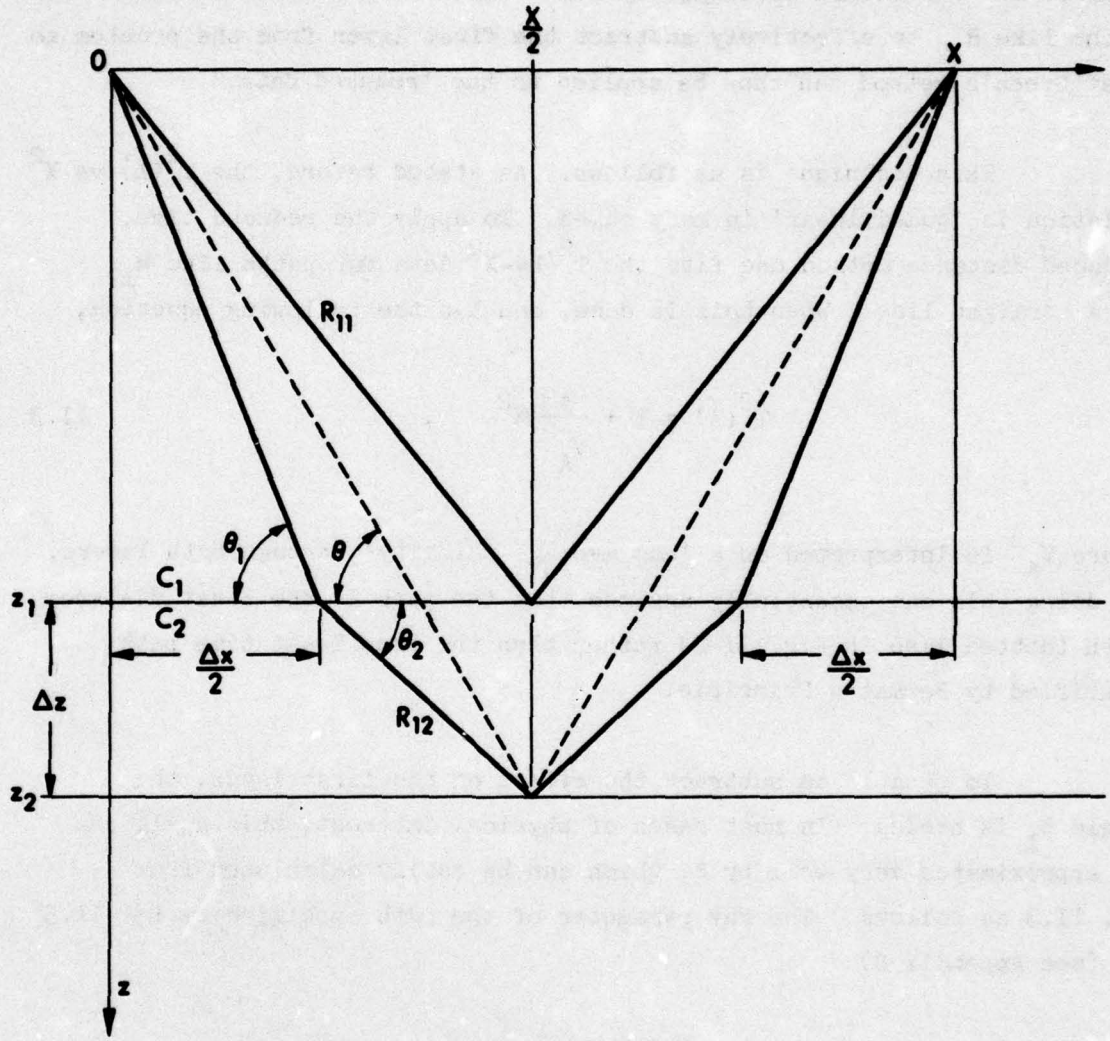

FIGURE II.2
REFLECTION RAY PATHS FOR TWO FLAT, ISOVELOCITY LAYERS OF THICKNESSES z_1 AND Δz AND VELOCITIES C_1 AND C_2

ARL - UT
AS-76-1171
SRR - DR
11 - 2 - 76

there is no longer a linear relationship between $T^2(X)$ and X^2. However, in many cases of physical interest, this linear relationship is very nearly preserved. The method developed by Dix[3,4] uses information obtained from paths like R_{12} to effectively subtract the first layer from the problem so that Green's method can thus be applied to the 'reduced data.'

This technique is as follows. As stated before, the $T^2(X)$ vs X^2 relation is 'quasilinear' in many cases. To apply the reduced time, reduced distance method one fits the $T^2(X)$-X^2 data for paths like R_{12} to a straight line. When this is done, one has the following equation,

$$T^2(X) = B + \frac{1}{V_A^2} X^2 \quad , \qquad \text{II.3}$$

where V_A^2 is interpreted as a 'rms average velocity' through both layers. In doing this one essentially assumes that the path is the least distance path (dotted line in Fig. II-2) rather than the true least time path specified by Fermat's Principle.

To be able to subtract the effect of the first layer, the angle θ_1 is needed. In most cases of physical interest, this angle can be approximated very well by θ, which can be easily calculated from Eq. II.3 as follows. The ray parameter of the path specified by Eq. II.3 is (see Appendix B)

$$p = \frac{dT(X)}{dX} = \frac{\cos \theta_1}{C_1} \quad .$$

Using Eq. II.3, one obtains

$$2T(X)\,\frac{dT(X)}{dX} = \frac{2X}{V_A^{\,2}} \quad ,$$

$$p = \frac{dT(X)}{dX} = \frac{X}{T(X)V_A^{\,2}} \simeq \frac{\cos\theta_1}{C_1} \quad ,$$

or

$$\cos\theta_1 \simeq \frac{C_1 X}{T(X)V_A^{\,2}} \qquad \text{II.4}$$

Once θ_1 is known, those portions of the time and horizontal distance of path R_{12} which lie within layer 1 may be calculated and subtracted from the original T and X values for paths R_{12}. This is done in the following manner. From Fig. II.2, the contribution to X from layer 1 is ΔX, where

$$\Delta X = \frac{2Z_1}{\tan\theta_1} \qquad \text{II.5}$$

The contribution to the time resulting from layer 1 is Δt, where

$$\Delta t = \frac{2Z_1}{\sin\theta_1 C_1} \qquad \text{II.6}$$

and

$$\frac{2Z_1}{\sin\theta_1}$$

is the length of the path R_{12} which lies in layer 1. When ΔX and Δt are known, the first layer may be subtracted to leave the reduced time and reduced distance values T_R and X_R, which are given by

$$T_R = T - \Delta t$$

$$X_R = X - \Delta X \quad . \qquad \text{II.7}$$

If the T and X values for R_{12} paths are reduced, the problem has essentially been transformed to a one layer problem. This being the case, the relation between T_R^2 and X_R^2 should be a linear one given by

$$T_R^2 = (T_o)_R^2 + \frac{1}{C_2^2} X_R^2 \quad , \qquad \text{II.8}$$

where $(T_o)_R^2$ is the vertical reflection time through layer 2 and C_2 is the interval velocity in layer 2. Once $(T_o)_R$ and C_2 are known, the thickness of layer 2 may be determined by the following equation,

$$\Delta Z_2 = \frac{C_2 (T_o)_R}{2} \qquad \text{II.9}$$

This method is best illustrated by considering an example. Figure II.3 depicts the T versus X curves for a two-layer situation in which the first layer has a thickness and velocity of 500 m and 1500 m/sec and the second has a thickness of 200 m and an initial sound speed of 1365 m/sec which increases linearly with a gradient of 2 sec^{-1}. These curves were generated from a ray tracing program, PROBE,[12] which was developed at ARL/UT by Terry Foreman.

The top curve of Fig. II.3 results from R_{12}-type paths, whereas the bottom one results from R_{11}-type. The T^2 versus X^2 plot for the top curve is shown in Fig. II.4. A least squares fit yields $V_A^2 = 2.314$ km^2/sec^2. If Eqs. II.4, II.5, II.6, and II.7 are used along with X and T values obtained from Fig. II.3, then Table II.1 may be computed. The X_R and T_R values that were computed are then fit by least squares (see Fig. II.5) to yield

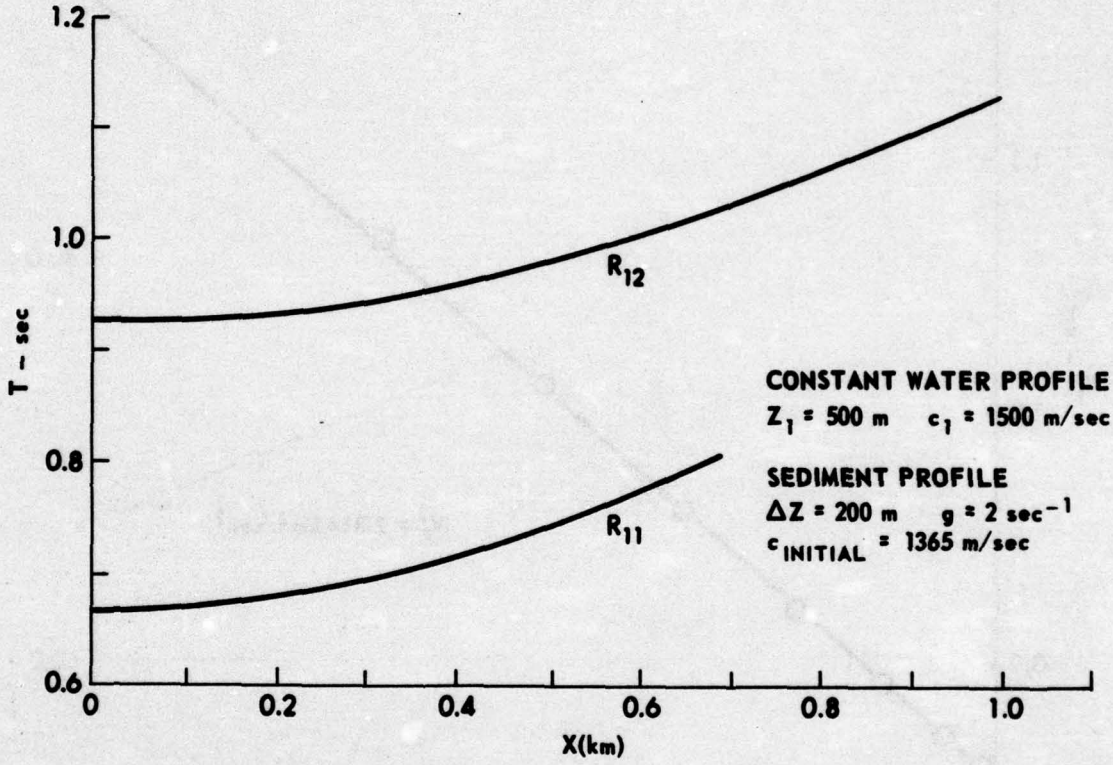

FIGURE II.3
TIME versus DISTANCE CURVE FOR A TWO LAYER CONFIGURATION

ARL - UT
AS-76-1172
SRR - DR
11 - 2 - 76

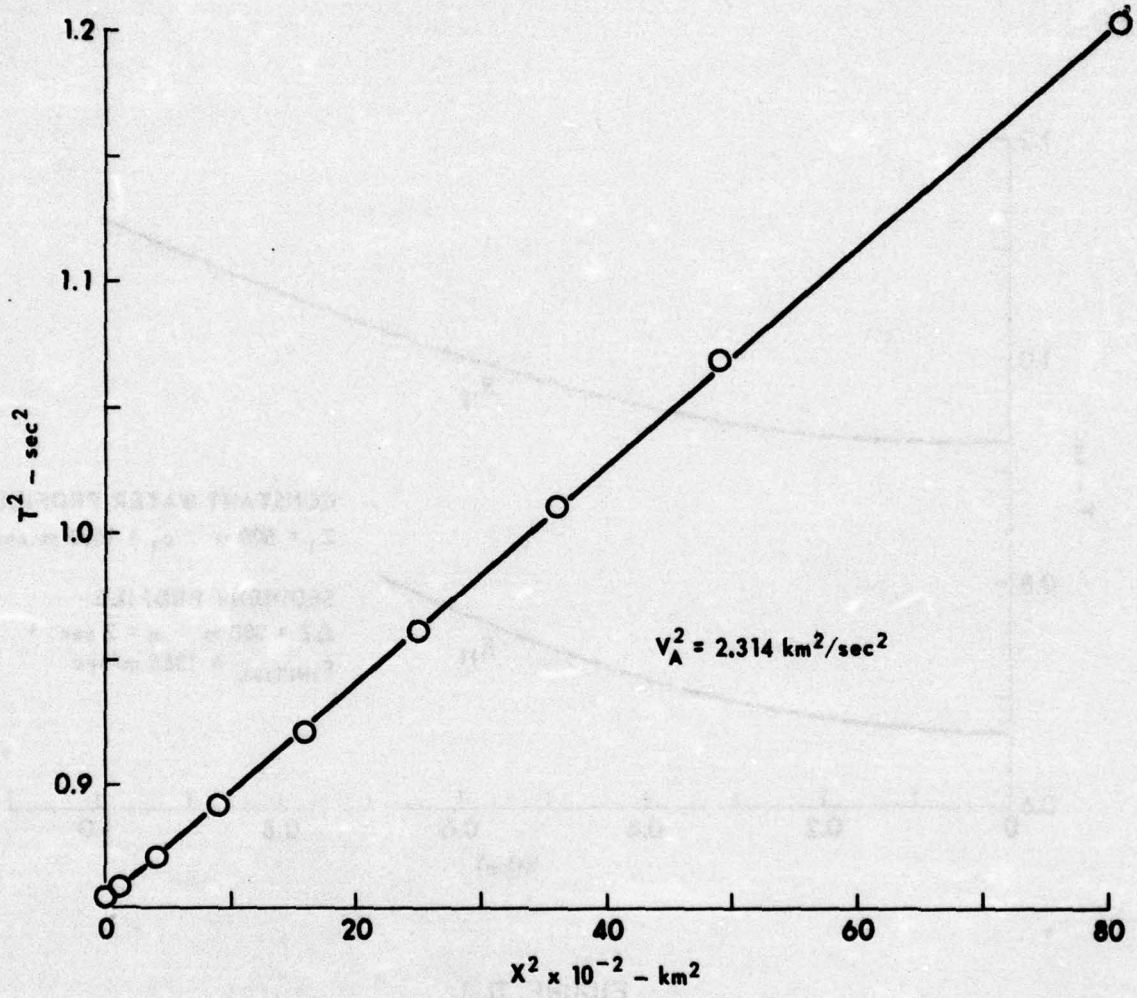

FIGURE II.4
T^2 versus X^2 GRAPH FOR R_{12} CURVE OF FIGURE II.3

ARL - UT
AS-76-1173
SRR - DR
11 - 2 - 76

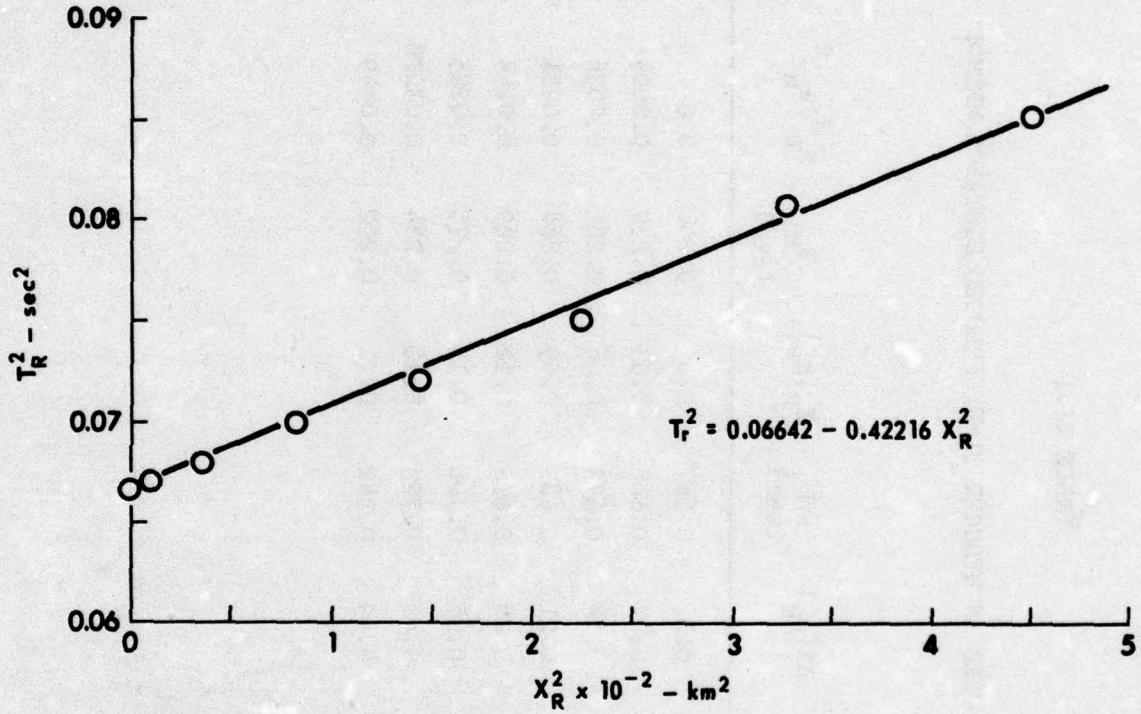

FIGURE II.5
T^2 versus X^2 GRAPH FOR REDUCED DATA OF FIGURE II.4

ARL - UT
AS-76-1174
SRR - DR
11 - 2 - 76

TABLE II.1

QUANTITIES USED IN REDUCED TIME, REDUCED DISTANCE METHOD

$X(k_m)$	T (sec)	θ_1 (deg)	$\Delta X(k_m)$	ΔT (sec)	$X_R(k_m)$	T_R (sec)	$X_R^2(k_m)^2$	T_R^2 (sec^2)
0.0	0.925	90.00	0.0	0.667	0.0	0.258	0.0	0.0667
0.1	0.927	85.99	0.07	0.668	0.03	0.259	0.0009	0.0669
0.2	0.934	82.02	0.14	0.673	0.06	0.261	0.0036	0.0680
0.3	0.945	78.12	0.21	0.681	0.09	0.264	0.0081	0.0695
0.4	0.961	74.35	0.28	0.692	0.12	0.269	0.0144	0.0722
0.5	0.981	70.71	0.35	0.706	0.15	0.275	0.0225	0.0755
0.6	1.007	67.28	0.42	0.723	0.18	0.284	0.03276	0.0808
0.7	1.034	63.97	0.49	0.742	0.21	0.292	0.0449	0.0853

$$T_R^2 = 0.06642 + 0.42216\, X_R^2 \quad . \qquad \text{II.10}$$

From Eqs. II.8, 9, and 10 one obtains

$$\Delta Z = \frac{(0.06642/0.42216)^{1/2}}{2} = 0.198 \text{ km}$$

$$C_2 = \left(\frac{1}{0.42216}\right)^{1/2} = 1.539 \text{ km/sec} \quad .$$

The actual values of ΔZ and C_2 are 200 m and 1561 m/sec, where the interval velocity of layer 2 was calculated from Eq. A.6.

This reduced time, reduced distance method can be extended to the case where there are more than two layers by a repeated application of the method. For example, if three layers are being considered, the velocities in the first two layers could be found using the techniques developed in this section. The knowledge of these two velocities and the ray parameter would allow the first two layers to be subtracted off, again leaving a one-layer problem that is easily handled. In this manner, the method may be extended to the n-layer case.

2. The Small Range Method

Although the method just discussed gives good results in most situations, it is relatively hard to use since a large number of X and T values must usually be reduced. Dix[3,4] developed an approximation which is valid for small range values and gives good results. This approximation is derived as follows.

From Fig. II.2, the following geometrical relations may be obtained for path R_{12},

$$X_1 = 2Z_1 \cot \theta_1 = C_1 T_1 \cot \theta_1 \quad , \qquad \text{II.11}$$

$$X_2 = 2(Z_2 - Z_1) \cot \theta_2 = C_2 T_2 \cot \theta_2 \quad ,$$

$$X = X_1 + X_2 \quad ,$$

where X_i is the contribution to the range resulting from layer i and T_i is the vertical two-way travel time thickness of layer i. If the range values are small compared to the thicknesses of the layers, i.e.,

$$X << Z_1 + \Delta Z \quad ,$$

then the cotangents of the angles may be approximated with the cosines. This substitution yields

$$X_1 + X_2 \simeq C_1 T_1 \cos \theta_1 + C_2 T_2 \cos \theta_2$$

$$\simeq C_1^2 T_1 \frac{\cos \theta_1}{C_1} + C_2^2 T_2 \frac{\cos \theta_2}{C_2} \quad .$$

But by Snell's Law,

$$\frac{\cos \theta_1}{C_1} = \frac{\cos \theta_2}{C_2} \quad ;$$

hence

$$X_1 + X_2 \simeq \left(C_1^2 T_1 + C_2^2 T_2 \right) \frac{\cos \theta_1}{C_1} \quad .$$

Substitution for $\cos \theta_1$ from Eq. II.4 yields

$$X = X_1 + X_2 \simeq \left(C_1^2 T_1 + C_2^2 T_2\right) \frac{X}{T(X) V_A^2} \quad ,$$

or as $X \to 0$,

$$V_A(0)^2 \left(T_1 + T_2\right) = \left(C_1^2 T_1 + C_2^2 T_2\right) \quad , \qquad \text{II.12}$$

where $V_A(0)^2$ is the slope of the T^2 versus X^2 plot for R_{12} paths in the limit of small range values and $T(0) = T_1 + T_2$.

This method will now be applied to the same example considered in the preceding section. From Fig. II.4, the slope of the T^2 versus X^2 curve for small range values is found to be $V_A^2 = 2.314$ km^2/sec^2. The velocity in the first layer is assumed to be known and is $C_1 = 1.5$ km/sec. From Fig. II.3 the vertical two-way time thicknesses of layers 1 and 2 may be measured to give

$$T_1 = 0.6668 \text{ sec} \quad ,$$

$$T_2 = 0.2577 \text{ sec} \quad .$$

Equation II.12 may now be solved for the layer velocity, C_2.

$$C_2^2 = \frac{V_A^2(0)(T_1 + T_2) - C_1^2 T_1}{T_2} \quad ,$$

$$C_2^2 = 2.3593 \text{ km}^2/\text{sec}^2 \quad .$$

$$C_2 = 1.575 \text{ km/sec} \quad .$$

This velocity compares favorably with the results of the previous method (C_2=1.539 km/sec) and the value calculated from Eq. A.6 (C_2=1.561 km/sec). The thickness of the layer may be computed as follows,

$$\Delta Z = \frac{C_2 T_2}{2} = 0.203 \text{ km} \quad .$$

This result is also in good agreement with the true value of 0.200 km.

The small range approximation considerably reduces the effort required to calculate interval velocities while having very little effect on the results. This method is very well suited for work in the field since the results can be obtained quickly using graphical techniques.

This method may also be used in the n-layer case. By mathematical induction, Eq. II.12 may be extended to the n-layer case to give

$$V_{A_n}^2 \sum_{i=1}^{n} T_i = \sum_{i=1}^{n} C_i^2 T_i \quad . \qquad \text{II.13}$$

For the n-1 layer case, Eq. II.13 is

$$V_{A_{n-1}}^2 \sum_{i=1}^{n-1} T_i = \sum_{i=1}^{n-1} C_i^2 T_i \quad .$$

The interval velocity of the nth layer is therefore

$$C_n^2 = \frac{V_{A_n}^2 \sum_{i=1}^{n} T_i - V_{A_{n-1}}^2 \sum_{i=1}^{n-1} T_i}{T_n} \quad ,$$

where T_i is the two-way vertical time through the ith layer, and $V_{A_n}^2$ is the reciprocal slope of the T^2 versus X^2 curve for the nth reflector.

3. Dürbaum's Analysis

This final version of the $T^2(X)$ method is a method developed by Dürbaum[5] in 1954. The material used in this report, however, was taken from a paper by Clay and Rona[13] (1965), because it provided a good summary of the method in English.

Dürbaum's method is a higher order method. Instead of fitting travel time data to a quadratic function of X, the data is fit to a fourth order polynomial in X, i.e.,

$$T_j^2(X) = A_0(j) + A_1(j)X + A_2(j)X^2 + A_3(j)X^3 + A_4(j)X^4 \quad . \qquad \text{II.14}$$

The subscript j refers to reflection times from the jth layer and $T_j(X)$ refers to a two-way reflection time rather than a two-way time thickness. The added first, third, and fourth power terms in Eq. II.14 allow layer configurations of a more complex nature to be treated. One important case that can be treated by Eq. II.14 is the one in which the subbottom layers are inclined at a small angle with respect to the surface layer (see Fig. II.6). The coefficients may be expressed in terms of the physical and geometrical parameters of the layered configuration as follows,

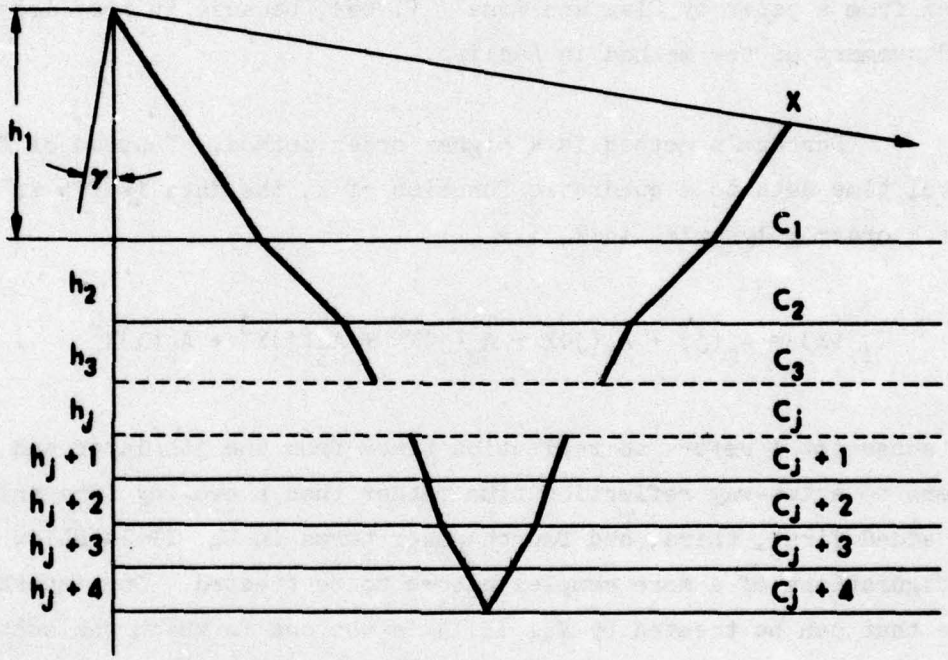

FIGURE II.6
CONFIGURATION FOR SLOPING SUBBOTTOM LAYERS
(AFTER CLAY AND RONA)

ARL - UT
AS-76-1175
SRR - DR
11 - 2 - 76

$$A_o(j) = \left[T_j(0)\right]^2 \quad ,$$

$$A_1(j) = -2T_j(0)\,\frac{\sin\gamma}{C_1} \quad ,$$

$$A_2(j) = \frac{\sin^2\gamma}{C_1^{\,2}} + \frac{T_j(0)\cos^2\gamma}{A_{1j}} \quad ,$$

$$A_3(j) = -\frac{\sin\gamma\cos^2\gamma}{C_1 A_{1j}}\left(1 - \frac{C_1^{\,2}T_j(0)}{A_{1j}}\right) \quad ,$$

$$A_4(j) = \frac{\cos^4\gamma}{4\,A_{1j}^{\,2}}\left[1 - \frac{T_j(0)\,B_{1j}}{A_{1j}^{\,2}} - 4\tan^2\gamma\left(1 - \frac{C_1^{\,2}T_j(0)}{A_{1j}}\right)\right] \quad ,$$

$$A_{1j} = \sum_i^j C_m^{\,2}\left[T_m(0) - T_{m-1}(0)\right] \quad ,$$

$$B_{1j} = \sum_i^j C_m^{\,4}\left[T_m(0) - T_{m-1}(0)\right] \quad .$$

To apply this version, as with the others, it is necessary to know the layer velocities and vertical travel times for each layer above the one in question. When these are known, along with the fitting coefficients $A_i(j)$, it is possible to calculate the layer velocity of the layer in question plus the angle of inclination of the subbottom layers, γ. (Notice that when $\gamma=0$, the $A_1(j)$ and $A_3(j)$ terms are zero.)

If the fourth power term is neglected and if an angle of inclination of zero is considered, Dürbaum's method reduces to the small range method. In practice, Dürbaum's method is most useful when sloping bottom layers are present. When the subbottom is not sloping, very little is gained by including the higher power terms. For more details concerning the application of this method, consult Clay and Rona[13] (1965).

4. Limitations of the $T^2(X)$ Methods

The main factor which causes the $T^2(X)$ methods to break down is the violation of the conditions assumed when deriving the equations to be used. The most apparent condition which is violated is the isovelocity assumption. When dealing with physical situations, the isovelocity condition is almost never satisfied. Hamilton[14] has determined that sediment velocity gradients generally range between 0.5 and 2.0 sec^{-1}; hence errors are introduced because the paths through the layers are curved rather than straight. In very thick nonhomogeneous layers, this can render the $T^2(X)$ methods useless (Bryan,[6] 1974).

As a further example, consider a configuration like the one in Fig. II.2, where the top layer is a relatively thick water layer and the bottom a much thinner sediment layer. Let τ_1 be the time associated with path R_{11} and τ_2 be the time associated with R_{12}. If the isovelocity assumption introduced an absolute error of Δt in the time of path R_{11}, then the relative error in the water is of order $\Delta t/\tau_1$. If the data concerning the second layer are calculated, the relative error in these data is of order

$$\frac{\Delta t}{\tau_2 - \tau_1} \quad \frac{\Delta t}{\tau_1} \frac{\tau_1}{\tau_2 - \tau_1} \quad .$$

Since $\tau_1/\tau_2-\tau_1$ is roughly proportional to h_1/h_2, where h_i is the thickness of layer i, the absolute error of the data in the bottom is magnified by

the ratio of the thicknesses of the two layers. In most cases the water layer has a fairly slowly changing velocity profile, but if the water layer were very thick and the sediment layer very thin, it is conceivable that the absolute error of the reduced data could be of the same magnitude as the data itself. These are the conditions under which the $T^2(X)$ methods break down.

The examples considered in this section yielded results for layer velocities and thicknesses that were within 1.5% of the standard values. These results are quite good, but it should be remembered that the data that were analyzed were obtained from computer ray tracing programs. When dealing with real world data, the quality of the data will usually preclude attaining results as good as these.

B. Ray Parameter Method

The ray parameter method (RPM) developed by Bryan[6] (1974), uses an alternative approach in the analysis of travel time data. Rather than compare paths of the same shot position, the RPM compares paths of the same ray parameter p. This approach yields a solution for the velocity in subbottom layers which is independent of the velocity structure above this layer.

1. Derivation of the Method[6]

A ray path is characterized by a constant ray parameter, p, which is defined by Snell's Law to be

$$p = \frac{\cos \theta(z)}{c(z)} \quad . \qquad \text{II.15}$$

The angle θ is the angle that the ray makes with the horizontal, i.e., the grazing angle.

For an incremental travel time dt, the following equations may be written (see Fig. II.7),

$$dz = c(z)dt \sin\theta(z) \quad ,$$

$$dx = c(z)dt \cos\theta(z) \quad . \qquad \text{II.16}$$

If Eq. II.15 and the trignometric relation

$$\cos^2\theta + \sin^2\theta = 1$$

are used, Eqs. II.16 may be written as

$$dz = \left(1-p^2c^2\right)^{1/2} cdt \quad ,$$

$$dx = c^2pdt = pc\left(1-p^2c^2\right)^{-1/2} dz \quad , \qquad \text{II.17}$$

where $cdt = dz/\left(1-p^2c^2\right)^{1/2}$ has been used to obtain the second of Eq. II.17. The travel time and range as a function of p may be obtained by rearranging and integrating Eqs. II.17 to yield

$$t(p) = 2\int_o^z \frac{dz}{c\sqrt{1-p^2c^2}}$$

$$x(p) = 2\int_o^z \frac{pc\,dz}{\sqrt{1-p^2c^2}} \qquad \text{II.18}$$

To transform Eqs. II.18 into usable forms, consider the configurations pictured in Fig. II.8. The object of the method is to measure the interval velocity of the layer bounded by $z=z_1$ and $z=z_1+\Delta z$.

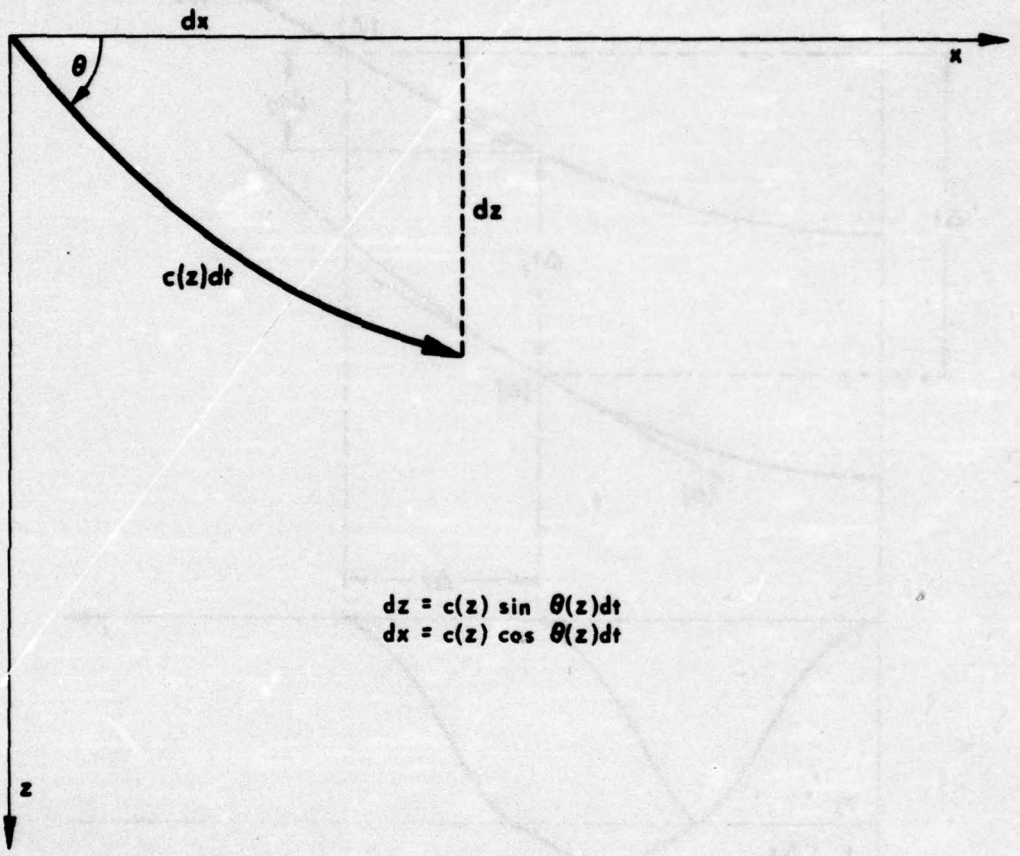

FIGURE II.7
GEOMETRY SHOWING THE RELATION OF dx AND dz TO dt

ARL - UT
AS-76-1176
SRR - DR
11 - 2 - 76

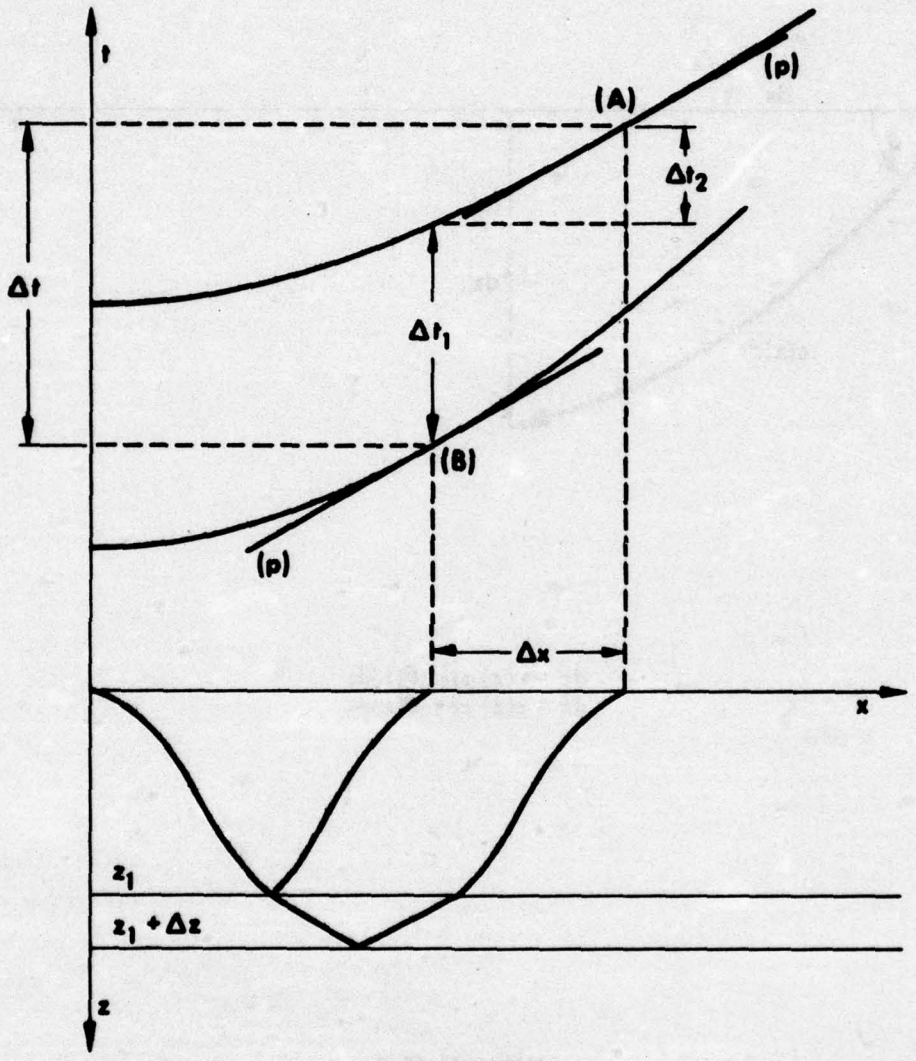

FIGURE II.8
GEOMETRY FOR RAY PARAMETER METHOD OF INTERVAL VELOCITY ANALYSIS
(AFTER BRYAN)

ARL - UT
AS-76-1177
SRR - DR
11 - 2 - 76

The two paths pictured in the bottom half of Fig. II.8 give rise to the travel time curves in the top half. Both paths have the same ray parameter p. This is a very important point as will be seen shortly.

To calculate the layer velocity it is first necessary to evaluate Δt and Δx as functions of p. This is done as follows,

$$\Delta t(p) = 2 \int_{z_1}^{z_1+\Delta z} \frac{dz}{c(z)\left(1-p^2c^2\right)^{1/2}} \quad ,$$

$$\Delta x(p) = 2 \int_{z_1}^{z_1+\Delta z} \frac{pc(z)dz}{\left(1-p^2c^2\right)^{1/2}} \quad . \qquad \text{II.19}$$

The fact that paths with the same ray parameter are being considered means that p in Eqs. II.19 is constant. To evaluate Eqs. II.19 only one simplifying assumption need be made, that being that the layer bounded by z_1 and $z_1+\Delta z$ is isovelocity. If this assumption is made, the integrals in Eq. II.19 are readily evaluated to yield

$$\Delta t(p) = 2C_1^{-1}\left(1-p^2C_1^2\right)^{-1/2} \Delta z \quad ,$$

$$\Delta x(p) = 2pC_1\left(1-p^2C_1^2\right)^{-1/2} \Delta z \quad ; \qquad \text{II.20}$$

the quantity C_1 is used to denote the interval velocity of the layer in question.

Equation II.20 may now be solved for the interval velocity of the layer to give

$$C_1 = \sqrt{\frac{1}{p}\frac{\Delta x}{\Delta t}} \qquad \Delta z = \frac{C_1 \Delta t}{2}\sqrt{1 - p^2 C_1^2} \quad . \qquad \text{II.21}$$

The important thing about the RPM is that the velocity structure above $z=z_1$ has no bearing whatsoever, a consequence of analyzing paths having the same ray parameter. Since both paths have the same ray parameter, their paths in the region above $z=z_1$ are completely parallel and hence cancel totally when the integration is performed. The only region where isovelocity was assumed was in the layer to be analyzed. Therefore the RPM is inherently superior to the $T^2(X)$ method since it assumes isovelocity in all layers.

2. The Normal Method of Solution

To apply the RPM it is necessary to match the paths of two adjacent reflectors having the same values of p. The data to be analyzed will be travel time data and the ray parameter will vary along these curves. The parameter of a ray arriving at a particular range is the slope of the travel time curve at that range (see Appendix B). Hence, applying the RPM will involve calculating, numerically, the derivatives of travel time curves.

To see how the RPM is normally applied, consider Fig. II.8. The first step in the analysis is to find two places on the T-X curves which have the same slope. This will involve calculating numerical first derivatives on each curve and matching them. Let points A and B in Fig. II.8 denote two such points. Next, the differences in times and distance between the points can be determined. If p, Δx, and Δt are known, the interval velocity C_1 may then be calculated by the first of Eqs. II.21. When C_1 is known, Δz may be calculated using the second

of Eqs. II.21. This procedure may be repeated for many different points and the results averaged to give the layer thickness and interval velocity.

Although the RPM is inherently superior to the $T^2(X)$ method, it is not without its shortcomings. When the layer to be analyzed becomes thin compared to the overlying layers, the RPM becomes unstable as does the $T^2(X)$ method. This instability arises for different reasons though.

When a thin layer underlying a thick layer is to be analyzed, the T-X curves for the bounding interfaces will be practically parallel over the entire range of x. This means that points A and B in Fig. II-9 will have almost the same range values, and this introduces an instability because Δx is so small that the error associated with its measurement is of the same order as Δx itself. Bryan has determined that these instabilities arise when the overlying layers are roughly 50 times the thickness of the layer to be measured. Fortunately, the RPM may be modified in such a manner as to remove the instability associated with small values of $\Delta x(p)$.

3. The Thin Layer Approximation

The thin layer approximation (TLA)[6] may be derived from Eqs. II.20. If one takes the ratio of $\Delta t(p)$ to $\Delta x(p)$, then the following equation is obtained,

$$\frac{1}{pC_1^2} = \frac{\Delta t(p)}{\Delta x(p)} \quad .$$

The next step is to express $\Delta t(p)$ as the sum of Δt_1 and Δt_2 as depicted in Fig. II.8. Hence,

$$\frac{1}{pC_1^2} = \frac{\Delta t_1}{\Delta x} + \frac{\Delta t_2}{\Delta x} \qquad \text{II.22}$$

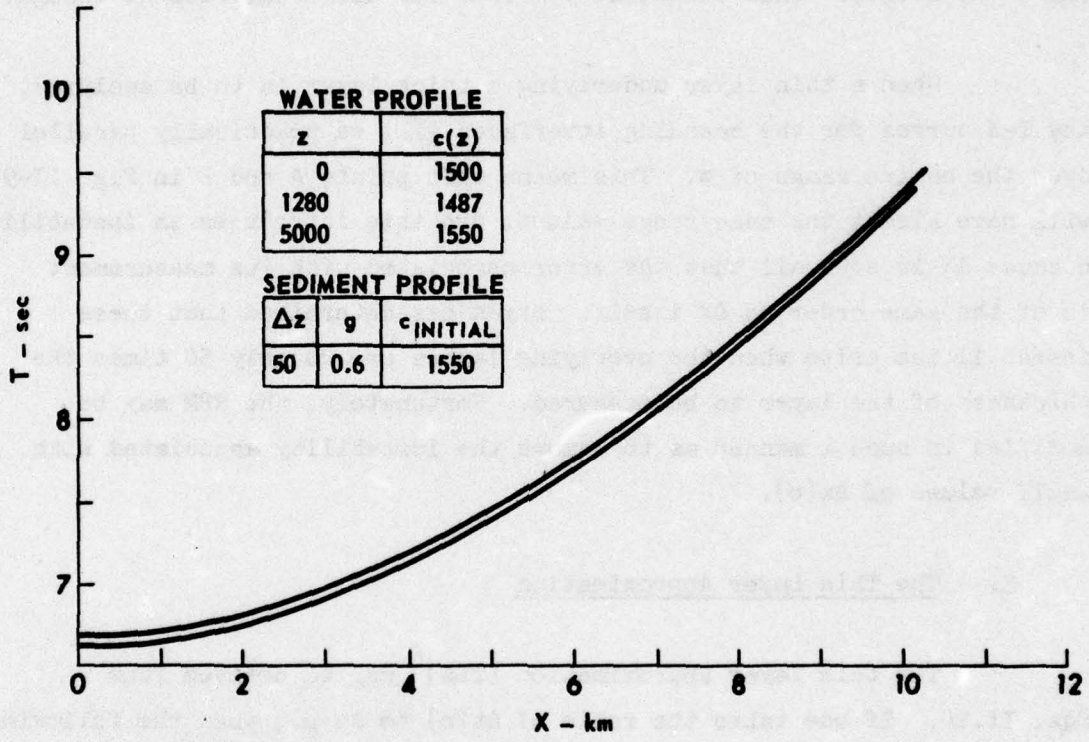

FIGURE II.9
TRAVEL TIME CURVE FOR A THICK WATER LAYER OVERLYING A THIN SEDIMENT LAYER

ARL - UT
AS-76-1178
SRR - DR
11 - 2 - 76

For large thickness ratios the travel time curves are straight and parallel across Δx; this implies that in the thin layer case $\Delta t_2/\Delta x$ approaches the slope p. If this substitution is made in Eq. II.22, one obtains

$$\frac{1}{pC_1^2} \simeq \frac{\Delta t_1}{\Delta x} + p \quad ,$$

$$\frac{1}{C_1^2} \simeq \frac{\Delta t_1}{\Delta x}\, p + p^2 \quad . \qquad \text{II.23}$$

If Δx is eliminated using Eq. II.20, the result is

$$p^2 = \frac{1}{C_1^2} - \frac{(\Delta t_1)^2}{4(\Delta z)^2} \quad . \qquad \text{II.24}$$

This equation does not depend on Δx and Δt_2, which become unstable in the case of thin layers. Equation II.24 is a linear equation in p^2 and Δt_1^2 and can be solved graphically for C_1 and Δt. It must be remembered that Δt_1 is the time difference between adjacent T-X curves at the same value of x.

How this method is applied can best be illustrated by considering an example. Figure II.9 depicts the travel time curves for a 2-layer configuration in which the first layer is a 5000 m water layer with a bilinear profile and the second layer is a sediment layer 50 m thick having an initial sound speed of 1550 m/sec and a constant gradient of 0.6 sec^{-1}. The bilinear water profile which was used is listed on Fig. II.9 as a set of depths and velocities. The profile is linear between these points. The data for the travel time curves in Fig. II.9 were obtained from ray tracing programs RANGER and PROBE[12] which were developed at ARL/UT by Terry L. Foreman. As is obvious from Fig. II.9, the two curves are essentially parallel throughout their range.

The first step in the TLA is to calculate the ray parameters for the top curve for a number of values of range. Table II.2 shows the X-T values of the top curve which were considered and the ray parameters calculated numerically with these values. The next step is to measure, from the T-X curves, the Δt_1 values at the range points considered. These are also included in Table II.2. The next step is to construct a graph of p^2 versus Δt_1^2; this graph is shown in Fig. II.10. The values used in the graph can be fit, using least squares, to a straight line. In the case being considered, the least squares fit yielded

$$p^2 = -102.941\ \Delta t_1^2 + 0.41682$$

where p is in seconds/kilometer and Δt_1 in seconds. A comparison with Eq. II.24 shows that

$$\frac{1}{C_1^2} = 0.41682 \quad ,$$

$$C_1 = 1.549 \text{ km/sec} \quad ,$$

and

$$\frac{1}{4(\Delta z)^2} = 102.941 \text{ km}^{-2} \quad ,$$

or

$$\Delta z = 49 \text{ m} \quad .$$

The true value for Δz is 50 m and the interval velocity calculated with Eq. A.6 is 1.565 km/sec. This agreement is remarkable considering the thickness ratio involved. But again it must be remembered that the data being analyzed was generated from a ray tracing program. This

TABLE II.2

THIN LAYER METHOD

X(km)	T(sec)	P(sec/km)	Δt_1(sec)
1	6.7096	0.065	0.0636
2	6.8065	0.128	0.0626
3	6.9651	0.188	0.0610
4	7.1812	0.243	0.0590
5	7.4499	0.293	0.0567
6	7.7656	0.337	0.0542
7	8.1229	0.376	0.0515
8	8.5166	0.410	0.0489
9	8.9418	0.439	0.0462

$P^2 = -102.94\ \Delta t_1^{\ 2} + 0.41682$

$C_1 = 1549$ m/sec

$\Delta z = 49$ m

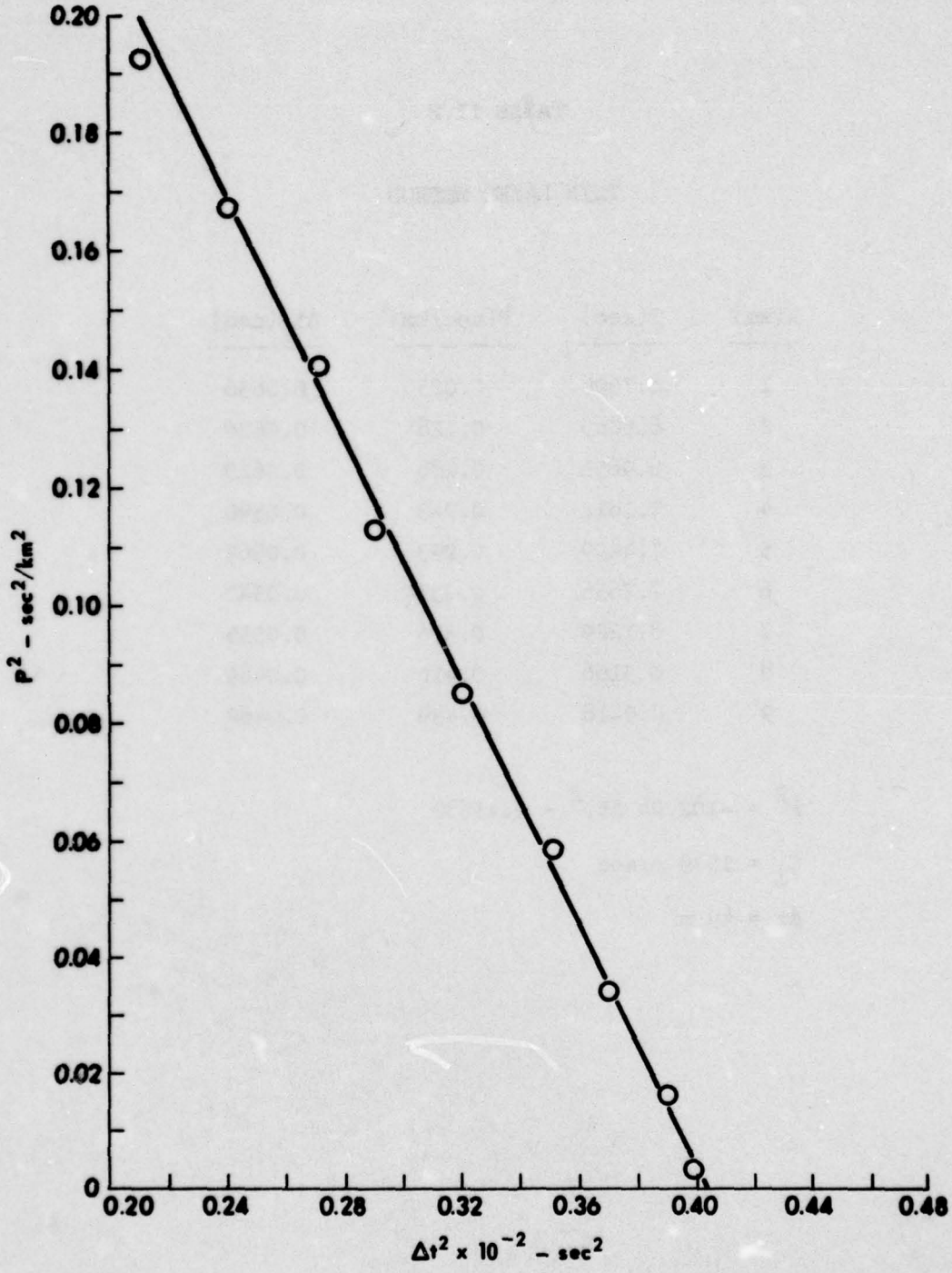

FIGURE II.10
P^2 versus Δt^2 GRAPH USED IN RAY PARAMETER METHOD

ARL - UT
AS-76-1179
SRR - DR
11 - 2 - 76

degree of precision is almost never realized when using real data. Bryan has determined that the TLA can give good results for thickness ratios of up to 500:1.

4. Sound Speed Gradient Information from the RPM*

In the derivation of the RPM it is necessary to assume that the layer to be analyzed is isovelocity. When nonhomogeneous layers are considered, the velocity obtained by the RPM is interpreted as the layer velocity and no information about the inhomogeneities is obtained.

There exists the possibility that the RPM may be used to obtain information about sound speed gradients in a layer through the use of a nomogram which gives possible combinations for C_o, Δz, and g. The quantity C_o is the velocity at the top of the layer, Δz is the layer thickness, and g is the constant sound speed gradient in the layer, the sound speed having been assumed to be $C(Z)=C_o+g z$.

The RPM works with time differences for rays traveling through n and n+1 layers while the range is increasing between source and receiver. The Δt between two travel time curves changes with the range. At range zero ($\theta=90°$), the Δt can be caused by an infinite number of combinations of Δz, C_o, and g. There is, however, only one combination of the parameters which fulfills the Δt values over the entire range. In other words, Δt as a function of X is uniquely specified by Δz, C_o, and g.

The only problem is that over large ranges of X, travel time curves belonging to a number of different combinations of Δz, C_o, and g are physically indistinguishable. This effect is most noticeable for small and intermediate values of range. The reason for this is that in the relatively thinner sediment layers, the amount of time the ray spends

---

*The material discussed in this subsection is a summary of previous research done by Jan Dräger as a visiting scientist from West Germany.

in the layer is small compared to the total time along the ray path; hence the travel time curve is fairly insensitive to the sediment parameters. As the range is increased, the time spent in the sediment layer increases and the effect of the sediment parameters becomes more noticeable. Unfortunately at the longer ranges, the reflected arrivals are often hard to differentiate from various other arrivals such as refracted arrivals and refraction arrivals and multiple bounce arrivals.

As an example of this effect, consider Fig. II.11. These travel time curves were generated by an isovelocity water layer 5 km thick and a sediment layer 100 m thick with a constant sound speed of 1280 m/sec. For the ranges considered, these curves are indistinguishable from those produced with a sediment layer having the parameters listed in Table II.3, the water layer remaining the same. Of course there are a number of values in between producing identical curves too.

The insensitivity of travel time curves to the sediment parameters makes obtaining information about velocity gradients a difficult task. One approach to the problem is to construct a family of g versus C_o curves for differing values of layer thickness. These curves are produced by ray tracing programs which use a water velocity profile appropriate to the experimental conditions. Figure II.12 is an example of such a family of curves produced from the ARL program PROBE. The water layer used for this example was a layer 5000 m thick having a constant sound speed of 1500 m/sec.

In principle, if one knew the velocity at the top of a layer and its thickness, one could find g from a family of curves like those in Fig. II.12. If the layer in question is the first sediment layer, this is not unreasonable since devices such as ARL's in situ compressional wave profilometer,[1] used while taking shallow sediment cores, measures C_o and the gradient in the upper portions of the sediment layers. If, however, the layer in question does not share an interface with the water,

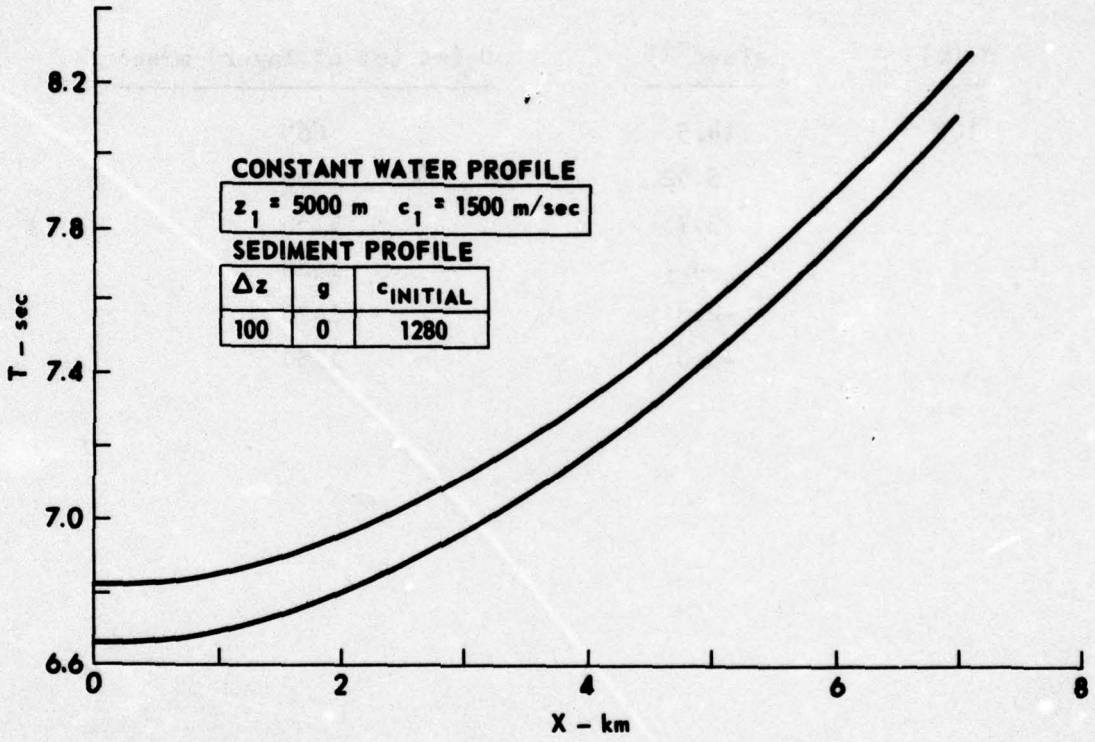

FIGURE II.11
TRAVEL TIME CURVES FOR A TWO LAYER CONFIGURATION USED TO SHOW INSENSITIVITY OF T-X CURVES TO SEDIMENT PARAMETERS

ARL - UT
AS-76-1180
SRR - DR
11 - 2 - 76

TABLE II.3

VALUES OF C_o, g, AND Δz PRODUCING IDENTICAL TRAVEL TIME CURVES

Δz(m)	g(sec^{-1})	C_o(at top of layer) m/sec
100	14.5	665
	5.92	1008
	3.75	1100
	-0-	1280
	-2.8	1426
	-5.0	1550

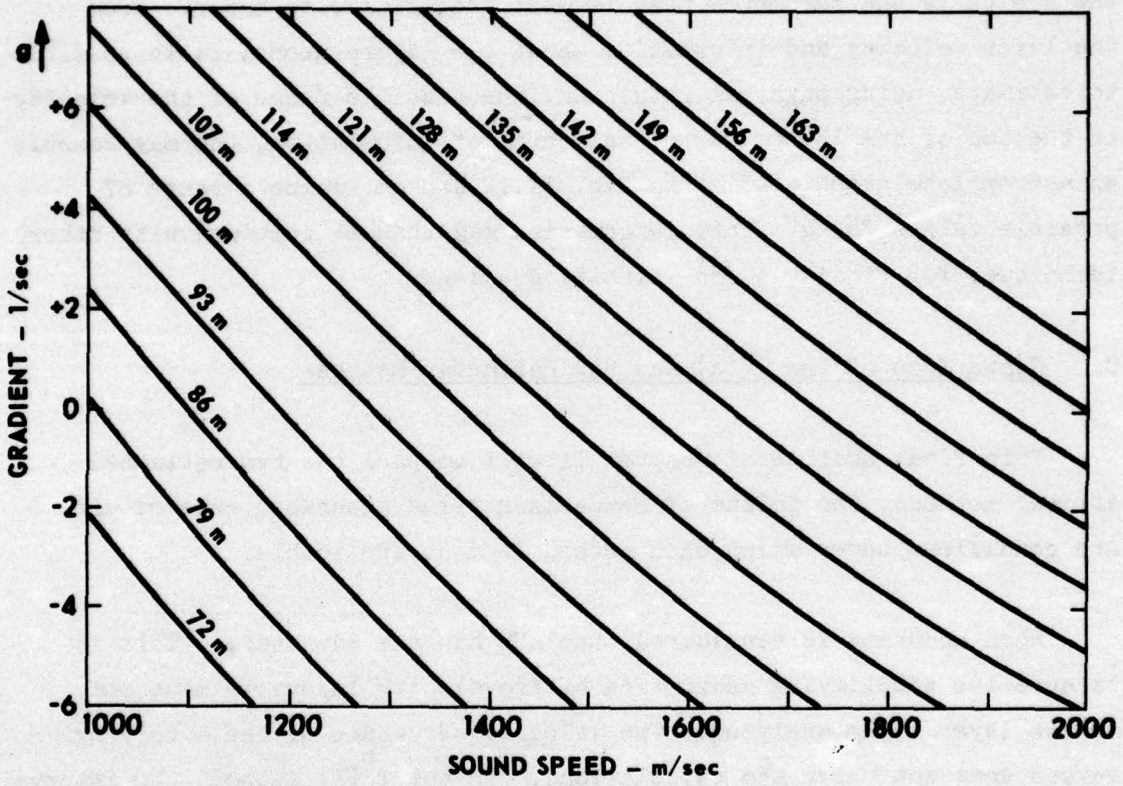

FIGURE II.12
g versus $c_{INITIAL}$ CURVES FOR DIFFERENT LAYER THICKNESSES

ARL - UT
AS-76-1181
SRR - DR
11 - 2 - 76

the velocity at the top of the layer is not usually known, which in turn makes it hard to pin down the value of g. It is possible, though, in a case like this to determine some upper and lower bound on the values of g. This is done in the following manner.

The thickness of a layer is usually known fairly well. In the RPM it is the parameter that is most insensitive to error. From the layer velocity and information about the layers above, it is possible to estimate, using physical intuition, the possible range of the velocity at the top of the layer. With these bits of information, one may consult an appropriate graph similar to Fig. II.12 and determine a range of possible values for g. This information may then be combined with other techniques for finding sound velocity gradients.

C. Comparison of the $T^2(X)$ and Ray Parameter Methods

This final section of Chapter II will compare the two reflected arrival methods, the points of comparison being accuracy, ease of use, and conditions under which each method is most applicable.

When accuracy is considered, the RPM has the advantage. This is because the simplifying assumption of isovelocity layers is made only in the layer being analyzed. The velocity structure of the overlying layers does not enter the calculations. In the $T^2(X)$ method, the interval velocity solution requires a knowledge of all overlying layers and these layers, which are assumed to be isovelocity, are added sources of error.

The $T^2(X)$ method may be improved when applied to situations in which the first layer is a thick water layer with a known velocity profile. If the water profile is known then ray tracing techniques can be used to more accurately determine the amount of time and range which results because of the water layer. This added step would greatly complicate the technique however.

When one considers ease of use, the $T^2(X)$ method has the advantage. The $T^2(X)$ method can be used with nothing more than a ruler, graph paper, and calculator, whereas the RPM requires a computer if quick results are needed; however, this is usually not an important problem since most profiling data is not analyzed in the field.

The conditions under which the $T^2(X)$ can be used with success are those involving layers with small thickness ratios. Bryan[6] has determined that for thickness ratios less than 15 the interval velocity in the thin layer is not sensitive to the velocity structure above. If one is dealing with small thickness ratios (shallow water, for example), then the $T^2(X)$ methods give good results quickly. Also, the $T^2(X)$ method as developed by Dürbaum is useful when sloping subbottom layers are considered.

The RPM can be applied to a wide range of layer configurations. The normal RPM can be used for thickness ratios up to 50:1. When thinner layers are encountered, the thin layer approximation may be used out to thickness ratios of 500:1. The ability to handle thin layers makes the RPM most useful when analyzing high resolution profiling data in which many thin reflecting horizons are observed.

Another condition for the RPM is that relatively continuous travel time data be available. This type of data is needed because a relatively fine mesh of T and X values is needed in order to calculate the derivatives required by the RPM.

III. ANALYSIS OF INTERVAL VELOCITY DATA

In the study of sound propagation in the ocean, whether ray theory or normal mode theory is used, one needs to detail, as closely as possible, the subbottom velocity profile. Unfortunately, the subbottom is the region which is the hardest to obtain information about. With the exception of coring data, the layer and velocity structure of the subbottom must come from the analysis of profiling data.

The method developed by Houtz et al.[7,8] will allow one to obtain the velocity profile of the subbottom from interval velocities calculated using the methods of Chapter II. For lack of a better name, this method will be referred to as the V(t) method, since it works with velocity as a function of one-way travel time. The small letter "t" will be used in the chapter to denote one-way travel time as opposed to a capital "T" used in the previous chapter to denote two-way time.

A. Derivation of the V(t) Method

The V(t) method is one in which interval velocities and travel times are used to construct an instantaneous velocity function, V(t), from which a gradient and a depth function can be obtained. The first step in the derivation of this method is to relate the interval velocities to the instantaneous velocities. In the V(t) method, the interval velocity of a layer is assumed to be the instantaneous velocity at the midpoint, in time, of that layer. Or, in other words, if a certain reflecting layer is bounded by one-way times t and $t+\Delta t$, then the interval velocity of the layer is assumed to be the instantaneous velocity at $t+\Delta t/2$. The assignment of the interval velocity to the instantaneous velocity at the midpoint in time is not entirely correct but Houtz et al. in their paper, "Velocity of Deep-Sea Sediments from Sonobouy Data,"[7] show that this assumption is generally in error by much less than 50 m/sec.

The V(t) method is implemented by fitting the interval velocities to a continuous third order polynomial in t, the one-way travel time, i.e.,

$$V(t) = A + Bt + Ct^2 + Dt^3 \quad . \qquad \text{III.1}$$

A continuous velocity function is used in Eq. III.1, even though velocity discontinuities are quite common, because one is dealing with instantaneous velocities at the midpoints of layers. Profiling techniques do not provide enough information to handle velocity discontinuities which would occur at the layer boundaries between adjacent interval velocities; the effect is that any velocity discontinuities that might be present are smoothed out. An example of this effect will be shown later in this chapter.

A depth function may be obtained from Eq. III.1 by integrating with respect to t to give

$$H(t) = At + \frac{1}{2} Bt^2 + \frac{1}{3} Ct^3 + \frac{1}{4} Dt^4 \quad . \qquad \text{III.2}$$

A gradient function may be obtained from Eq. III.1 in the following manner. If V(t) is written as

$$V(t) = \frac{dH(t)}{dt} \quad ,$$

then the gradient as a function of t is formed from the following ratios

$$g(t) = \frac{dV(t)}{dH(t)} = \frac{\frac{dV(t)}{dt}}{\frac{dH(t)}{dt}} = \frac{\frac{dV(t)}{dt}}{V(t)}$$

or

$$g(t) = \frac{B + 2Ct + 3Dt^2}{A + Bt + Ct^2 + Dt^3} \quad . \qquad \text{III.3}$$

Once the coefficients A, B, C, and D are known, the depth and gradient as a function of t are easy to calculate.

If a layer is bounded by one-way times t and $t+\Delta t$, then the layer thickness, ΔZ, may be found using the following,

$$\Delta Z = H(t+\Delta t) - H(t) \quad . \qquad \text{III.4}$$

The gradient of this same layer may be reasonably well approximated by the gradient function evaluated at the midpoint in time of this layer, i.e.,

$$g \simeq g(t + \tfrac{1}{2}\Delta t) \quad . \qquad \text{III.5}$$

If a continuous velocity profile through the subbottom is desired, i.e., V as a function of H, it may be obtained from Eqs. III.1 and III.2 by forming pairs of velocity and depth values for the same values of t.

At ARL/UT, a slightly different V(t) method has been used. A computer program written by Terry Foreman fits the interval velocities and the times using the cubic spline technique,[15] rather than using least-squares to fit them to a third order polynomial. The cubic spline method is one in which a cubic equation like Eq. III.1 is fit between each pair of velocity-time values. Instead of one set of fitting coefficients, there are a number of sets of fitting coefficients, each set being used between a particular pair of adjacent velocity-time values. To evaluate the sets of coefficients, each cubic spline is required to match the adjacent splines with continuous first and second derivatives. The end result of this procedure is a velocity function which is smoother and has less abrupt behavior than one obtained by least squares.

B. An Example of the V(t) Method

As an example of the V(t) method, consider the case of four subbottom layers underlying a 5000 m water layer having a bilinear profile. Table III.1 lists the parameters of the subbottom layers and the water layer. The subbottom profile of this example has gradient discontinuities across the layer interfaces but the sound velocities are continuous.

Figure III.1 depicts the computer generated T-X curves for the example. Since the thickness ratios are large, the ray parameter method, using the thin layer approximation, was employed to determine the interval velocities, layer thicknesses, and vertical travel times. These values are listed in Table III.2. For comparison sake, the actual layer thicknesses and the layer velocities calculated from Eq. A.6 are included in parenthesis.

Before applying the V(t) method, one needs to form a set of values for the interval velocity versus one-way travel time to the midpoints, in time, of the four subbottom layers. These values are listed in Table III.3. The one-way times are referenced to the interface between the water and the first subbottom layer, i.e., t=0 refers to the top of the first subbottom layer.

The set of velocity-time values is next used as input to the ARL/UT spline fit program. This program determines the instantaneous velocity function, the depth function, and the gradient function and prints them in table form for a fine mesh of t values. In this example, the value of instantaneous velocity at the top of the first layer, i.e., t=0, is assumed to be known and is included in the fitting procedure. The program also generates Calcomp plots of the instantaneous velocity function and the velocity as a function of depth. These plots are given in Figs. III.2 and III.3.

TABLE III.1

Water Profile

Depth (m)	Sound Velocity (m/sec)
0	1500
1280	1487
5000	1550

Subbottom Profile

Subbottom Layer No.	Thickness (m)	Constant Gradient (sec^{-1})	Initial Sound Velocity (m/sec)
1	100	0.5	1550
2	100	1.0	1600
3	100	1.5	1700
4	100	2.0	1850

TABLE III.2

LAYER PARAMETERS CALCULATED BY THE THIN LAYER APPROXIMATION OF THE RAY PARAMETER METHOD

Subbottom Layer No.	ΔZ (m)	Interval Velocity (m/sec)	2-Way Vertical Travel Time (sec)
1	99 (100)	1560 (1575)	0.1270
2	101 (100)	1660 (1650)	0.1212
3	100 (100)	1779 (1774)	0.1127
4	101 (100)	1957 (1949)	0.1027

TABLE III.3

INTERVAL VELOCITY AS A FUNCTION OF ONE-WAY TIME

Interval Velocity (m/sec)	One-Way Time to Midpoint of Layer (sec)
1560	0.03175
1660	0.09381
1779	0.15228
1957	0.20613

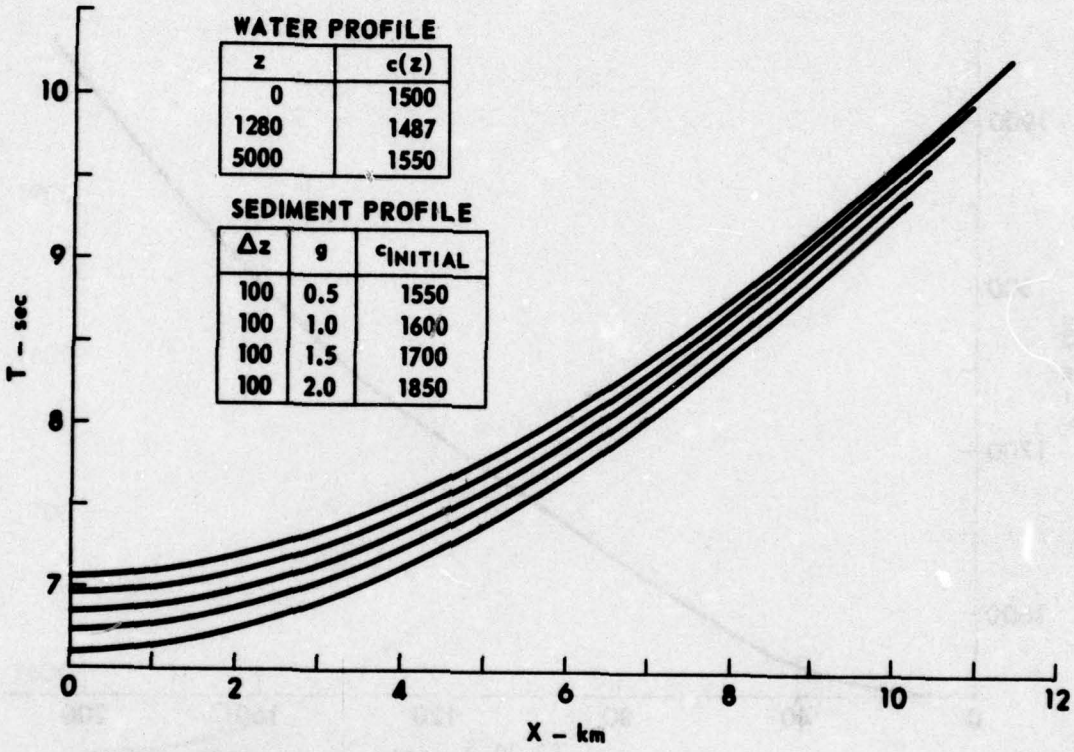

FIGURE III.1
TRAVEL TIME CURVES FOR A THICK WATER LAYER OVERLYING FOUR THIN SEDIMENT LAYERS

ARL - UT
AS-76-1182
SRR - DR
11 - 2 - 76

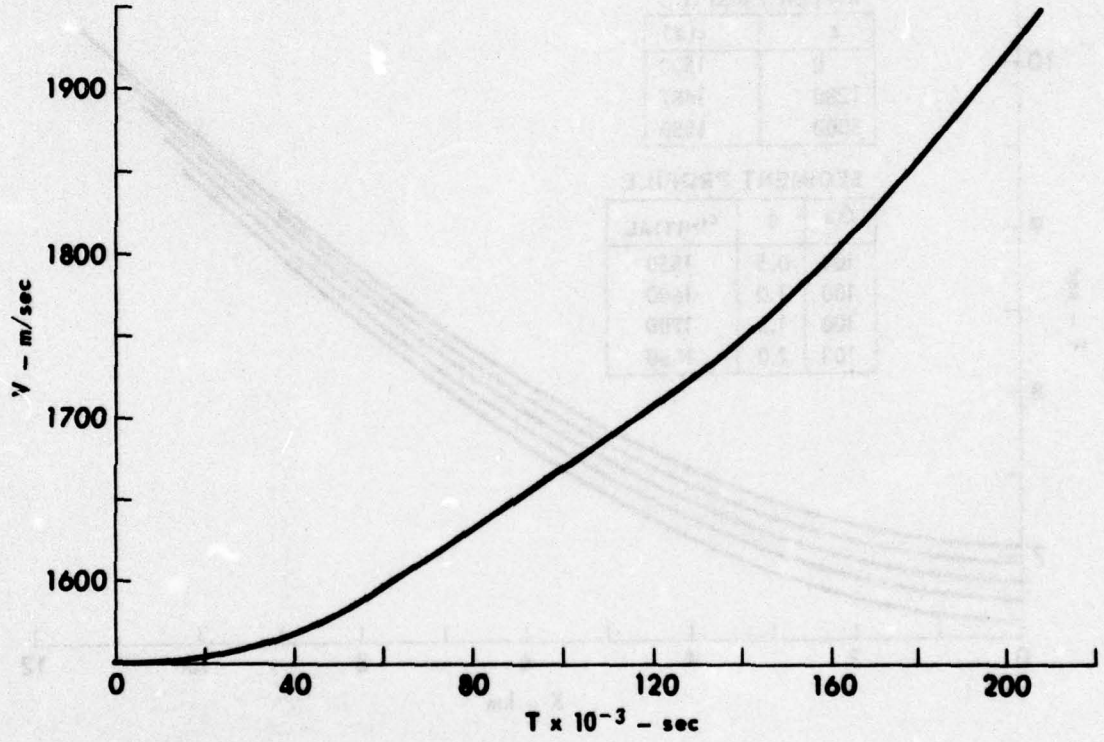

FIGURE III.2
INSTANTANEOUS VELOCITY AS A FUNCTION OF ONE-WAY TIME OBTAINED FROM INTERVAL VELOCITIES

ARL - UT
AS-76-1183
SRR - DR
11 - 2 - 76

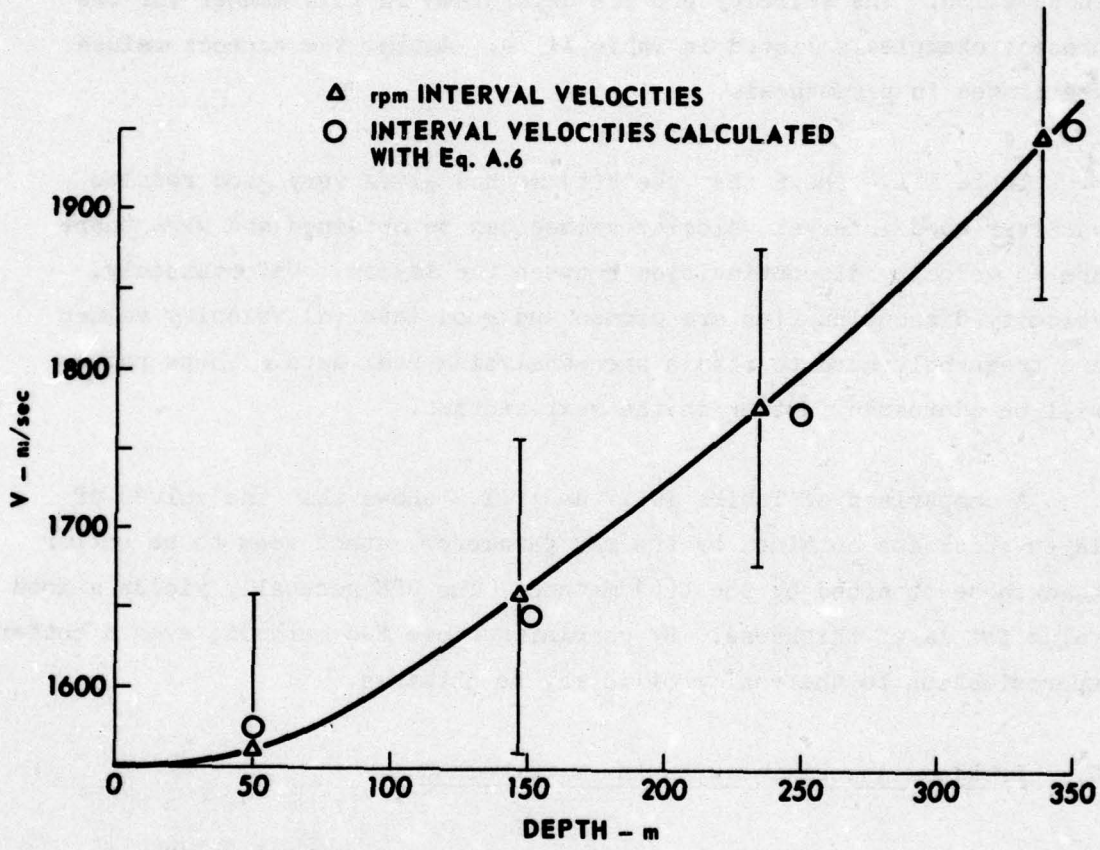

FIGURE III.3
SUBBOTTOM VELOCITY PROFILE OBTAINED BY V(t) METHOD

ARL - UT
AS-76-1184
SRR - DR
11 - 2 - 76

From the table of velocity, depth, and gradient values it is possible to reconstruct the subbottom profile. The layer thickness and layer gradient may be approximated by Eqs. III.4 and III.5, while the velocity at the top of each layer may be approximated by the instantaneous velocity function evaluated at the one-way time to the top of the layer in question. The velocity profile determined in this manner for the present example is listed in Table III.4. Again, the correct values are listed in parenthesis.

Table III.4 shows that the V(t) method gives very good results whenever good interval velocity values can be obtained and when there are no velocity discontinuities between the layers. Unfortunately, velocity discontinuities are common and good interval velocity values are frequently hard to obtain when analyzing real data. These points will be addressed further in the next section.

A comparison of Tables III.2 and III.4 shows that the values of layer thickness obtained by the ray parameter method seem to be better than those obtained by the V(t) method. The RPM generally yields a good value for layer thickness. By combining these two methods, even a better approximation to the real profile may be obtained.

C. Problems Associated with the V(t) Method

This section discusses problems which arise when the V(t) method is being employed, the problem due to velocity discontinuities and the effect of measurement errors on the results of the V(t) method.

1. Velocity Discontinuities

As seen in the example of Section B, when no velocity discontinuities are present the V(t) method is capable of reconstructing the subbottom velocity profile quite well. When velocity discontinuities

TABLE III.4

VELOCITY PROFILE RECONSTRUCTED FROM V(t) METHOD

Subbottom Layer No.	Thickness (m)	Constant Gradient (sec^{-1})	Initial Sound Velocity (m/sec)
1	99.7 (100)	0.5 (0.5)	1550 (1550)
2	95.2 (100)	1.1 (1.0)	1602 (1600)
3	77.0 (100)	1.5 (1.5)	1716 (1700)
4	129.0 (100)	1.8 (2.0)	1862 (1850)

are present, certain problems in the V(t) method arise. These problems are best illustrated by considering two examples.

Consider two configurations, each having four subbottom layers. The velocity profiles of these subbottom layers are listed in Table III.5. The first configuration is one in which there are no velocity discontinuities between the layers. The second configuration is identical to the first with the exception that velocity discontinuities between the layers are allowed.

For the purposes of this illustration, it was not necessary to analyze travel time curves. Instead, the interval velocities and travel times to be used in the V(t) method were calculated using the equations of Appendix A. These calculated values are shown in Table III.6. As in the last example, these values were used in the spline fit program to compute instantaneous velocity, depth, and gradient functions. The subbottom profiles reconstructed from the results of this program are listed in Table III.7.

A comparison of Tables III.5 and III.7 shows that, in the continuous case, the V(t) method reproduces the subbottom profile quite well, with the exception of the thicknesses of the last two layers which are in error by about 13%. The gradient values and the interval sound velocities were reproduced quite accurately.

The discontinuous case, however, did not work as well. The errors in the thickness values and in the initial sound speed all increased in the discontinuous case, though the initial sound speed proved to be less sensitive (maximum difference of 1.5%). The most pronounced differences were observed in the predicted gradients, the average percent difference being 30%. The reason for this difference is easily explained. As mentioned before, the V(t) method obtains a continuous instantaneous velocity function. Whenever velocity

TABLE III.5

SUBBOTTOM PROFILES FOR EXAMPLES OF SECTION III.C

Subbottom Layer No.	Thickness (m)	Constant Gradient (sec^{-1})	Initial Sound Speed (m/sec)
	Continuous Case		
1	100	1	1550
2	100	1	1650
3	100	1	1750
4	100	1	1850
	Discontinuous Case		
1	100	1	1550
2	100	1	1700
3	100	1	1820
4	100	1	1960

TABLE III.6

LAYER PARAMETERS CALCULATED USING THE RESULTS OF APPENDIX A

Subbottom Layer No.	Two-Way Vertical Travel Time (sec)	Interval Velocity (m/sec)	One-Way Midpoint Time (sec)
	Continuous Case		
1	0.1250	1600	0.03126
2	0.1177	1700	0.09192
3	0.1111	1800	0.14913
4	0.1053	1900	0.20322
	Discontinuous Case		
1	0.1250	1600	0.03126
2	0.1143	1750	0.09108
3	0.1070	1870	0.14639
4	0.0995	2009	0.19803

TABLE III.7

VELOCITY PROFILES RECONSTRUCTED FROM THEORETICAL VALUES OF INTERVAL VELOCITIES AND TRAVEL TIMES

Subbottom Layer No.	Thickness (m)	Constant Gradient (sec^{-1})	Initial Sound Speed (m/sec)
		Continuous Case	
1	98.5	1.006	1550
2	95.5	0.996	1651
3	87.1	1.004	1751
4	87.1	0.984	1851
		Discontinuous Case	
1	98.4	0.905	1550
2	93.4	1.379	1675
3	73.2	1.249	1812
4	119.4	1.429	1939

discontinuities are present, the interval velocity of a layer is larger than it would be if no discontinuities were present. Since the V(t) method does not recognize discontinuities, it reacts by predicting a larger value for the layer gradient to compensate for the higher interval velocity.

This brings up the question of whether velocity discontinuities can be detected using the V(t) method. The answer has to be, "sometimes." Anytime the V(t) method gives gradient values that seem unrealistically high, the expected range being 0.5 sec^{-1} to 2.0 sec^{-1},[14] one can suspect that a velocity discontinuity exists. In general, to determine the gradient more closely, one must use and combine as much information and as many methods as possible. For example, if velocity discontinuities are suspected, the V(t) method can be used to produce a 'first guess.' Well cores from geologically similar regions and possibly the gradient analysis discussed in Chapter II can then be used to revise the first guess. In this manner one can obtain a best possible guess of the velocity profile.

2. Effects of Measurement Errors

All of the data of the examples considered in this chapter were generated from a computer ray tracing program. It goes without saying that interval velocities calculated from actual data will have significant uncertainties associated with them, and these uncertainties will affect the subbottom velocity profiles.

Clay and Rona[13] indicate that the $T^2(X)$ method of interval velocity analysis produces uncertainties of the order of ±200 m/sec. It is expected that this uncertainty can be reduced to the order of ±100 m/sec by use of the ray parameter methods.

To get a feeling for the effect this uncertainty has on the gradient, consider the following simplified 'linear analysis.' Assume that one is attempting to determine the gradient in a single sediment layer having an initial sound speed of 1500 m/sec, a thickness of 300 m, and a constant gradient of 1 sec^{-1}. The equations derived in Appendix A yield an interval velocity value of 1648 m/sec and a two-way vertical travel time of 0.3646 sec, or a one-way time to the midpoint of 0.0912 sec (see Fig. III.4).

The depth coordinate of this interval velocity may be approximated by the product of interval velocity and one-way midpoint time [$Z \simeq (1648 \text{ in./sec})(0.0912 \text{ sec}) = 150.3$ m].

The simplified linear analysis mentioned above consists of calculating the linear slope between the two velocity depth values, (1500 m/sec, 0) and (1648 m/sec, 150.3 m). The result is

$$g \simeq \frac{(1648 - 1500) \text{ m/sec}}{150.3 \text{ m}} = 0.98 \text{ sec}^{-1} \quad .$$

If the 1500 m/sec velocity is assumed to be exact, and uncertainties of ±200 m/sec and ±5 m are assumed for the interval velocity and the depth coordinate, statistical analysis for the combination of errors for the above equation yields an uncertainty for g of about ±1.4 sec^{-1}. If the uncertainty of the interval velocity is taken to be ±100 msec, the uncertainty in g is reduced to ±0.8 sec^{-1}. Hence, errors in the measurement of interval velocities have a tremendous effect on the confidence one has in his results.

To see the possible effects of measurement errors on a multilayer case, consider Fig. III.3. In this figure, the conservative value for the uncertainty of the interval velocities, i.e., ±100 m/sec, is marked by the vertical bars centered on the interval velocity points calculated by the RPM. For comparison the interval velocities calculated

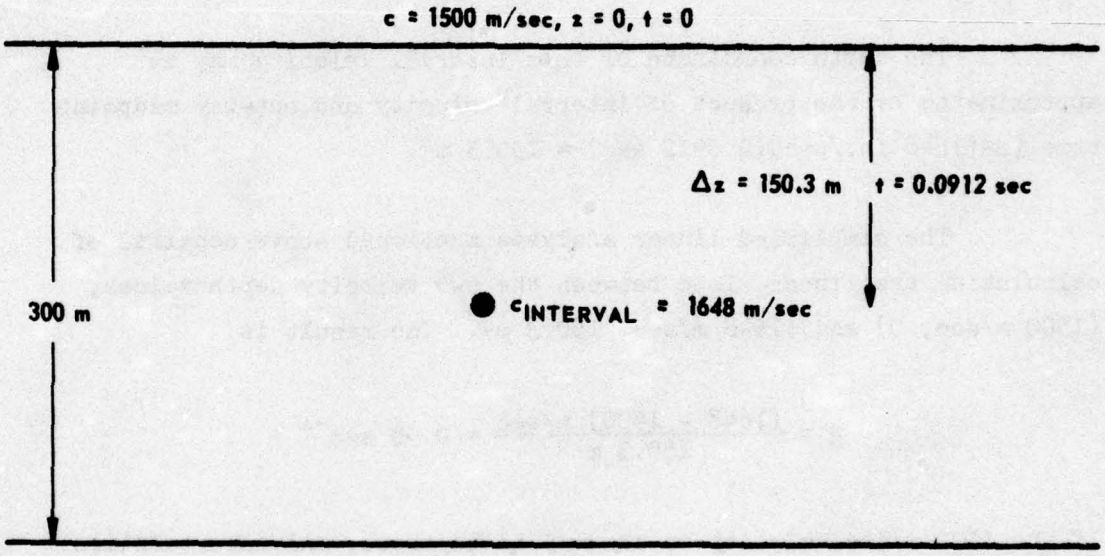

FIGURE III.4
LAYER CONFIGURATION USED TO DEMONSTRATE THE EFFECT OF MEASUREMENT ERRORS

ARL - UT
AS-76-1185
SRR - DR
11 - 2 - 76

using Eq. A.6 are also pictured. Needless to say, if the quality of the data was such as to make the interval velocities suspect, then one could, at best, only determine the general trend of the velocity profile.

IV. REFRACTED ARRIVAL METHODS

The two methods to be discussed in this chapter obtain the velocity profile in a single subbottom layer by techniques that employ the effects of refracted arrivals. The first method, used by Dicus,[9] works with travel times of the refracted arrivals. The second method, developed by Hanna,[10] calculates transmission loss due to energy refracted through the subbottom as a function of range.

Both these methods use the same model for the subbottom. The assumed bottom configuration is a single layer which has a pseudolinear velocity profile given by

$$C(Z) = \frac{C_o}{\sqrt{1 - \frac{2\beta Z}{C_o}}} \quad , \qquad \text{IV.1}$$

where C_o is the velocity at the top of the layer and β is the sound speed gradient at the surface of the layer ($\beta = C'(0)$).

A. Dicus' Method

Dicus' method is capable of determining the initial values of sound speed and gradient in a single layer through an analysis of the time differences berween arrivals that refract through the bottom and those that reflect from the top of the subbottom layer (see Fig. IV.1). Dicus' method is derived in the following manner.

1. Derivation

From Fig. IV.1, one may write the following expression for the time difference between paths 1 and 2,

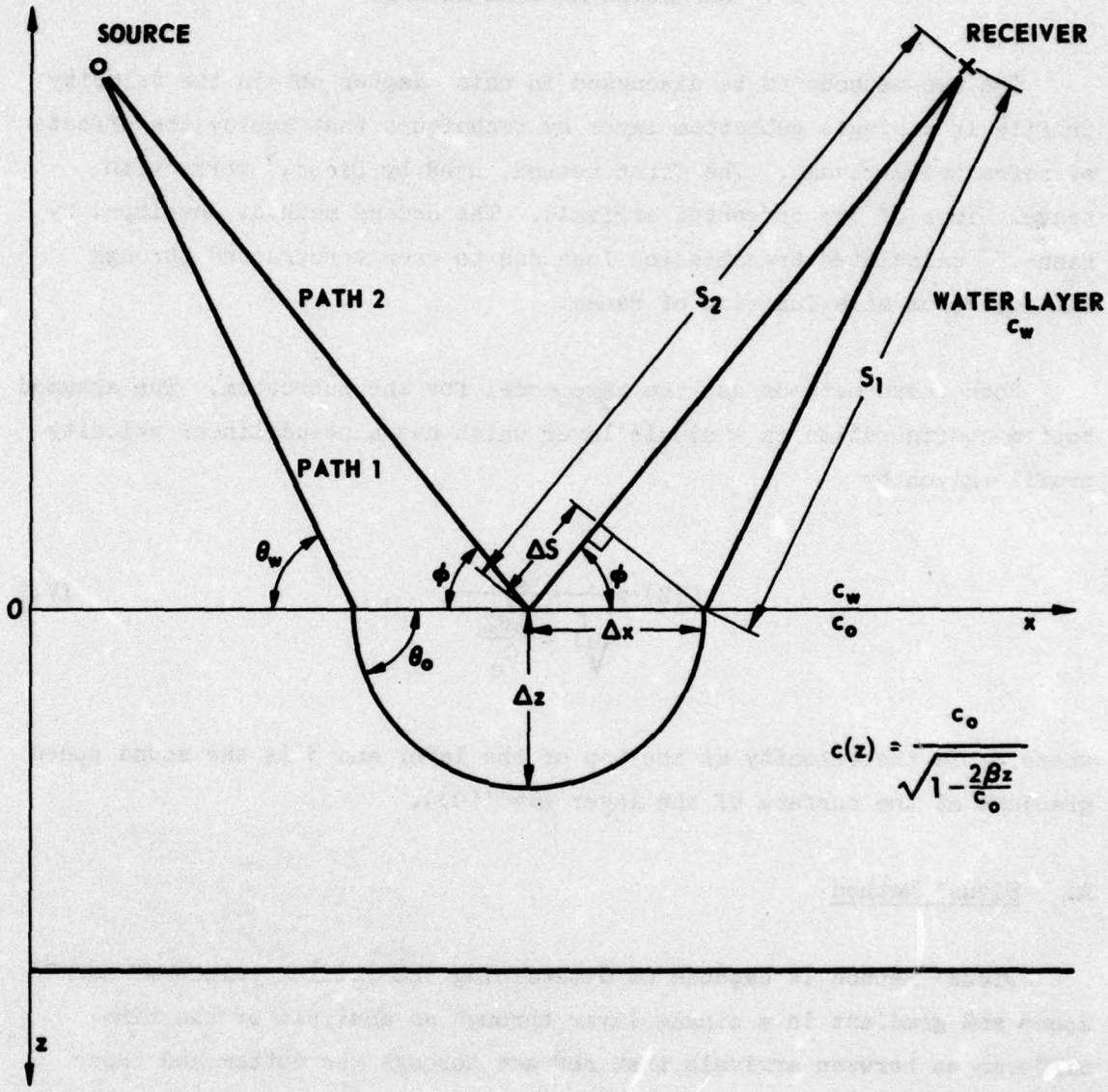

FIGURE IV.1
LAYER AND RAY PATH GEOMETRY CONSIDERED IN DISCUS' METHOD

ARL - UT
AS-76-1211
SRR - DR
11 - 2 - 76

$$\Delta\tau = \int_{\text{path 1}} \frac{ds}{C(Z)} - \int_{\text{path 2}} \frac{ds}{C(Z)} \quad . \qquad \text{IV.2}$$

The quantity ds is an incremental distance along the ray path. If the water layer is assumed to have a slowly varying velocity profile, then the water paths may be approximated by straight lines and Eq. IV.2 becomes

$$\Delta\tau = \int_{\text{path 1}} \frac{ds}{C(Z)} - \frac{2S_2}{C_w} \quad , \qquad \text{IV.3}$$

where C_w is the time averaged sound speed in the water.

From the geometry of Fig. IV.1, the integral in Eq. IV.3 may be written as

$$\int_{\text{path 1}} \frac{ds}{C(Z)} = \frac{2S_1}{C_w} + \int_{\text{sed.}} \frac{ds}{C(Z)} \quad , \qquad \text{IV.4}$$

where sed. refers to that portion of path 1 which lies in the sediment layer. Combining Eqs. IV.3 and IV.4, one obtains

$$\Delta\tau = \int_{\text{sed.}} \frac{ds}{C(Z)} - \frac{2\Delta S}{C_w} \quad , \qquad \text{IV.5}$$

with $\Delta S = S_2 - S_1$. If ΔS is approximated by $\Delta X \cos\phi$, Eq. IV.5 becomes

$$\Delta\tau = \int_{\text{sed.}} \frac{ds}{C(Z)} - \frac{2\Delta X \cos\phi}{C_w} \quad . \qquad \text{IV.6}$$

The integral in Eq. IV.6 may be written as

$$\int_{sed.} \frac{ds}{C(Z)} = 2 \int_{o}^{\Delta Z} \frac{dZ}{\sin \theta(Z)\, C(Z)} \quad , \qquad \text{IV.7}$$

where $dZ = ds \sin \theta(Z)$ has been used. The second integral in Eq. IV.7 is most easily evaluated by changing the variable of integration from Z to C(Z), the sound velocity in the sediment layer. This procedure yields

$$\int_{sed.} \frac{ds}{C(Z)} = \frac{2C_o^4}{\beta \cos \theta_o} \int_{C_o}^{C_o/\cos \theta_o} \frac{dC}{C^4(Z)\sqrt{\frac{C_o^2}{\cos^2 \theta_o} - C^2(Z)}} \quad ,$$

$$= \frac{2 \sin \theta_o}{3\beta} \left(1 + 2 \cos^2 \theta_o\right) \quad . \qquad \text{IV.8}$$

To obtain Eq. IV.8, the following relationships were used,

$$\frac{dC}{dZ} = \frac{\beta}{\left(1 - \frac{2\beta Z}{C_o}\right)^{3/2}} = \frac{\beta C^3(Z)}{C_o^3}$$

$$\sin \theta(Z) = \sqrt{1 - \cos^2 \theta(Z)} = \sqrt{1 - C^2(Z) \frac{\cos^2 \theta_o}{C_o^2}} \quad .$$

If Eq. IV.8 is substituted into Eq. IV.6 the following expression is obtained,

$$\Delta\tau = \frac{2 \sin \theta_o}{3\beta} \left(1 + 2 \cos^2 \theta_o\right) - \frac{2 \cos \phi}{C_w} \Delta X \quad . \qquad \text{IV.9}$$

To finish the evaluation of $\Delta\tau$, an expression for ΔX in terms of the sediment parameters is required. This expression is obtained as follows,

$$\Delta X = \int_{o}^{\Delta Z} \frac{dZ}{\tan\theta(Z)} = \int_{C_o}^{C_o/\cos\theta_o} \frac{C_o^{\,3} dC}{\tan\theta(Z)\beta\, C^3(Z)} \quad . \qquad \text{IV.10}$$

If one uses

$$\tan\theta(Z) = \frac{\sin\theta(Z)}{\cos\theta(Z)} = \frac{\sqrt{1 - \dfrac{C^2(Z)\cos^2\theta_o}{C_o^{\,2}}}}{\dfrac{C(Z)}{C_o}\cos\theta_o}$$

in Eq. IV.10, the result is

$$\Delta X = \frac{C_o^{\,3}}{\beta} \int_{C_o}^{C_o/\cos\theta_o} \frac{dC}{C^2\sqrt{\dfrac{C_o^{\,2}}{\cos^2\theta_o} - C^2}} = \frac{C_o \cos\theta_o \sin\theta_o}{\beta} \quad . \qquad \text{IV.11}$$

With Eq. IV.11, Eq. IV.9 becomes

$$\Delta\tau = \frac{2\sin\theta_o}{3\beta}\left(1 + 2\cos^2\theta_o\right) - \frac{2\cos\phi}{C_w}\,\frac{C_o\cos\theta_o\sin\theta_o}{\beta} \quad . \qquad \text{IV.12}$$

If the water layer is thick and the source depth shallow, the angle ϕ may be approximated well by the angle θw. This substitution in Eq. IV.12 yields

$$\Delta\tau = \frac{2 \sin \theta_o}{3\beta}\left(1 + 2 \cos^2 \theta_o\right) - \frac{2 \cos \theta_w}{C_w} \frac{C_o \cos \theta_o \sin \theta_o}{\beta} \quad . \qquad \text{IV.13}$$

From Snell's Law, $C_o \cos \theta_w / C_w$, may be replaced by $\cos \theta_o$ to give

$$\Delta\tau = \frac{2 \sin \theta_o}{3\beta}\left(1 + 2 \cos^2 \theta_o\right) - 2 \cos^2 \theta_o \frac{\sin \theta_o}{\beta}$$

$$= \frac{2 \sin \theta_o}{3\beta}\left(1 - \cos^2 \theta_o\right) = \frac{2}{3\beta}\left(1 - \cos^2 \theta_o\right)^{3/2} \quad . \qquad \text{IV.14}$$

Snell's Law may be used once again to yield

$$\Delta\tau = \frac{2}{3\beta}\left(1 - \frac{C_o^2}{C_w^2} \cos^2 \theta_w\right)^{3/2} \quad . \qquad \text{IV.15}$$

Equation IV.15 may be transformed into a form that can be solved graphically for C_o/C_w and β by making the following substitutions. Let $r=\cos^2 \theta_w$ and $s=(3\Delta\tau/2)^{2/3}$. With these changes of variables, Eq. IV.15 can be written as

$$s = \frac{1}{\beta^{2/3}} - \left\{\left(\frac{C_o}{C_w}\right)^2 r + 1\right\} \quad . \qquad \text{IV.16}$$

Equation IV.16 is a linear equation in s and r which can be solved for β and C_o/C_w graphically.

It is possible to obtain the simple expression in Eq. IV.16 because of the assumption of a pseudolinear profile. The pseudolinear profile does, however, have a few problems associated with it. At a

critical depth of $Z_{crit}=C_o/2\beta$, the pseudolinear profile is singular and as Z approaches Z_{crit} the velocity profile becomes physically unrealistic. This can have an effect on Dicus' method if one is analyzing data from thick subbottom layers. For this reason, when thick layers are present one should analyze that part of the data which has the smaller bottom angles, i.e., the shallower refracting rays.

If thin layers or shallow refracted rays are considered, the pseudolinear gradient parameter β should be nearly the same as the constant gradient g. From Eq. IV.1 in the limit of small values of the ratio $2\beta Z/C_o$, one may write

$$C(Z) = \frac{C_o}{\sqrt{1 - \frac{2\beta Z}{C_o}}} \xrightarrow[\frac{2\beta Z}{C_o} \to 0]{} C_o + \beta Z \quad .$$

Hence, in this limit, β should be very nearly equal to g, the linear gradient.

2. Example of Dicus' Method

To illustrate this method, consider a 2-layer configuration like the one pictured in Fig. IV.1. Let the top layer correspond to an isovelocity water layer with a sound speed (C_w) of 1500 m/sec and thickness of 5000 m. Let the subbottom layer be a layer 400 m thick with an initial sound velocity of 1550 m/sec and a constant gradient of $g=1.0\ sec^{-1}$. (The linear gradient is used in this example to show the correspondence between β and g and because the ray tracing programs used to generate the data of this example require that constant gradients be used.)

Table IV.1 lists the values of θ_w, $\Delta\tau$, s, and r which were obtained from the ARL ray tracing program RANGER. To simulate actual

TABLE IV.1

QUANTITIES USED IN THE APPLICATION OF DICUS' METHOD

Range (km)	θ_w (deg)	$\Delta\tau$ (sec)	$s = \left(\frac{3}{2}\Delta\tau\right)^{2/3}$ $\left(\text{sec}^{2/3}\right)$	$r = \cos^2 \theta_w$
15	37.999	0.1310	0.3380	0.6210
16	35.498	0.1051	0.2918	0.6628
17	33.334	0.0850	0.2531	0.6980
18	31.434	0.0690	0.2205	0.7280
19	29.749	0.0563	0.1925	0.7538
20	28.240	0.0461	0.1685	0.7761
21	26.879	0.0378	0.1476	0.7956
22	25.646	0.0311	0.1296	0.8127
23	24.521	0.0255	0.1135	0.8277
24	23.492	0.0209	0.0994	0.8411

$s = -1.0833\ r + 1.00974$

$s = 1.00974(-1.07284r+1)$

$\frac{C_o}{C_w} = 1.0358$

$\beta = 0.99\ \text{sec}^{-1}$

experimental conditions, the angle ϕ was used to approximate θ_w. Figure IV.2 depicts the graph of s versus r. From the very nearly linear relation between s and r, it would appear that in this case the pseudolinear profile well approximates the linear profile and that replacing θ_w by ϕ is justified.

A least-squares linear fit between s and r yields the following equation,

$$s = 1.00974(-1.07284r+1) \quad .$$

The values of C_o/C_w and β may be obtained from the above equation as follows,

$$\frac{C_o}{C_w} = \sqrt{1.07284} = 1.0358$$

$$\beta = \frac{1}{(1.00974)^{3/2}} = 0.99 \text{ sec}^{-1} \quad .$$

The actual values for these parameters are

$$C_o/C_w = 1550/1500 = 1.0333 \text{ and } g = 1 \text{ sec}^{-1} \quad .$$

The agreement between β and g indicates that the linear profile used to generate the data is well approximated by a pseudolinear profile.

3. Discussion

To be able to apply this method to experimental data two conditions must hold. First, it is necessary that one be able to identify refracted arrivals in the data. Sometimes this is not an

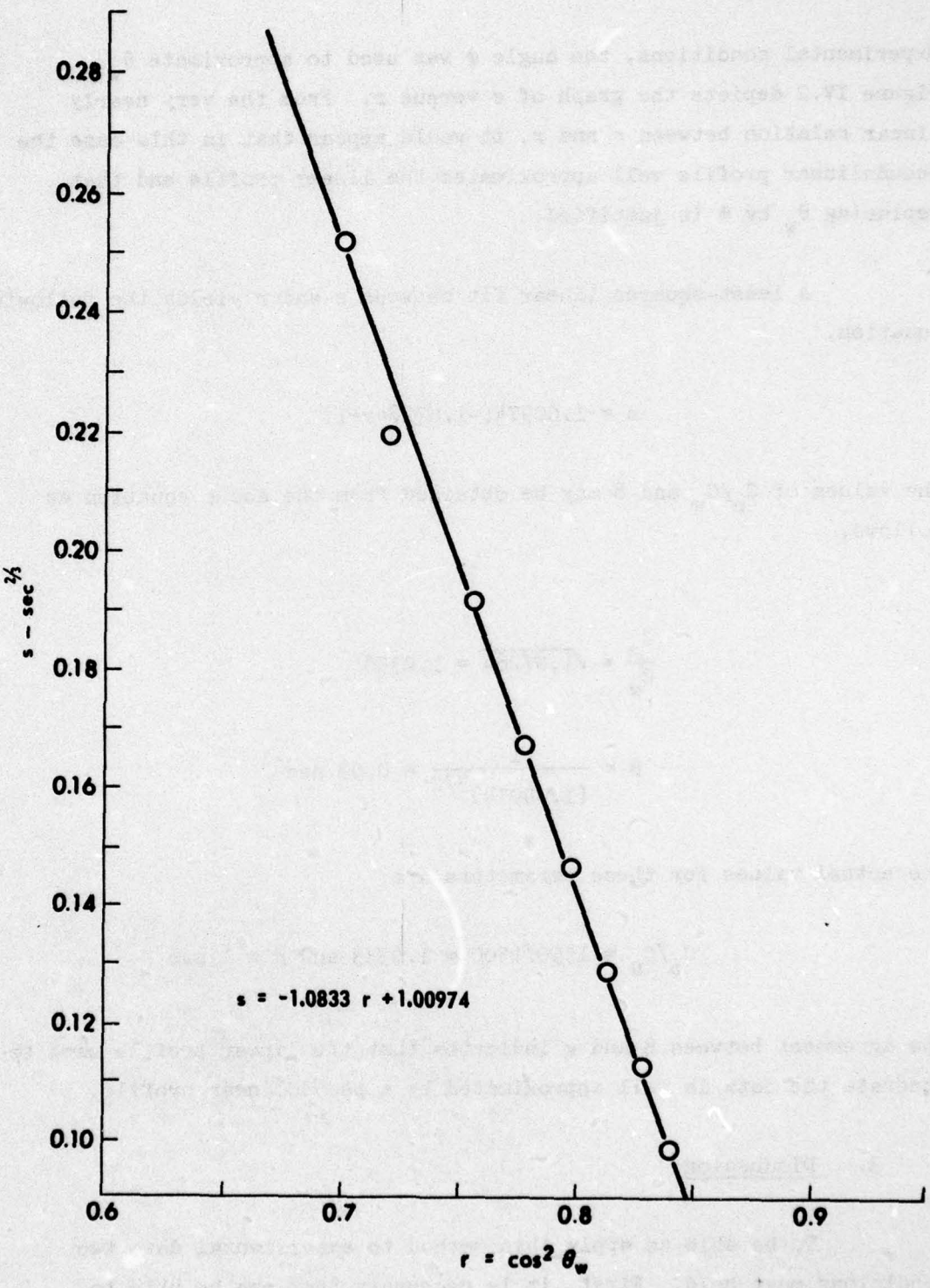

FIGURE IV.2

GRAPH OF $s = (\frac{3}{2}\Delta\tau)^{2/3}$ versus $r = \cos^2\theta_w$ USED IN DISCUS' METHOD

ARL - UT
AS-76-1212
SRR - DR
11 - 2 - 76

easy task. Usually, other preprocessing such as deconvolution processing is required before refracted arrivals can be identified. The second condition for the success of this model is that the angle θ_w be very nearly equal to ϕ (see Fig. IV.1). This is necessary because the angle θ_w cannot be determined beforehand without a knowledge of the subbottom profile. For this reason it is necessary to approximate θ_w with the angle ϕ, which can be determined if the water profile and horizontal range are known. In situations involving thick water layers and shallow sources this approximation is usually justified.

B. Hanna's Method

Hanna's Method is a unique method for determining subbottom velocity structures by analyzing nulls in a transmission loss curve for a bottomed receiver. This technique is described in J. S. Hanna's paper, "Short-Range Transmission Loss and the Evidence for Bottom-Refracted Energy."[10] This section is essentially a brief summary of Hanna's paper.

1. Proposed Method of Solution

Hanna's technique proposes to determine sediment velocity and gradient information from the interference structure exhibited by the transmission loss curve for a bottomed receiver over the range of the direct arrival. The range is restricted in this manner because, outside the range of the direct arrival, multibounce ray paths further complicate the transmission loss by adding more interference structure.

If there were no energy being returned from the bottom, the interference structure of the transmission loss should be accounted for quite well by the Lloyd's Mirror Effect. (The Lloyd's Mirror Effect is most noticeable when a shallow source is used and results from the interference of ray paths that are upgoing and downgoing at the source.) When energy is allowed to refract or reflect back into the water column,

the transmission loss curve will show added interference structure. Hanna's method proposes to identify interference nulls in transmission loss curves that arise because of refracted energy and to determine velocity and gradient information from the positions of these nulls.

2. Discussion of the Technique

The first assumption made when applying this method is that the energy incident on the bottom can be approximated by a plane wave and that a plane wave reflection coefficient may be used to describe the subbottom. Let the reflection coefficient be denoted by $R(\theta)$. This plane wave reflection coefficient is specified as a function of grazing angle and includes the effects of energy refracted in the bottom.

If a bottomed hydrophone is used to measure pressure levels, the amplitude as a function of grazing angle, $\alpha(\theta)$, may be specified as

$$\alpha(\theta) = A(\theta)[1+R(\theta)] \quad . \qquad \text{IV.17}$$

The function $A(\theta)$ is the amplitude of the incident plane wave and contains information concerning spreading loss and Lloyd's Mirror Effect. The term $1+R(\theta)$ contains information about interference between incident and reflected or refracted energy.

Before this method can be developed further, a model for the water and sediment layers must be specified. Hanna models the water layer as isovelocity and the subbottom as a sediment layer with a constant gradient overlying a solid isovelocity basement (see Fig. IV.3). For this configuration, the plane wave reflection coefficient may be approximated by the reflection coefficient for plane waves incident from an isovelocity half-space on the boundary of another half-space. This approximation should be good for thick sediment layers. The reflection coefficient[10] for this case may be written as

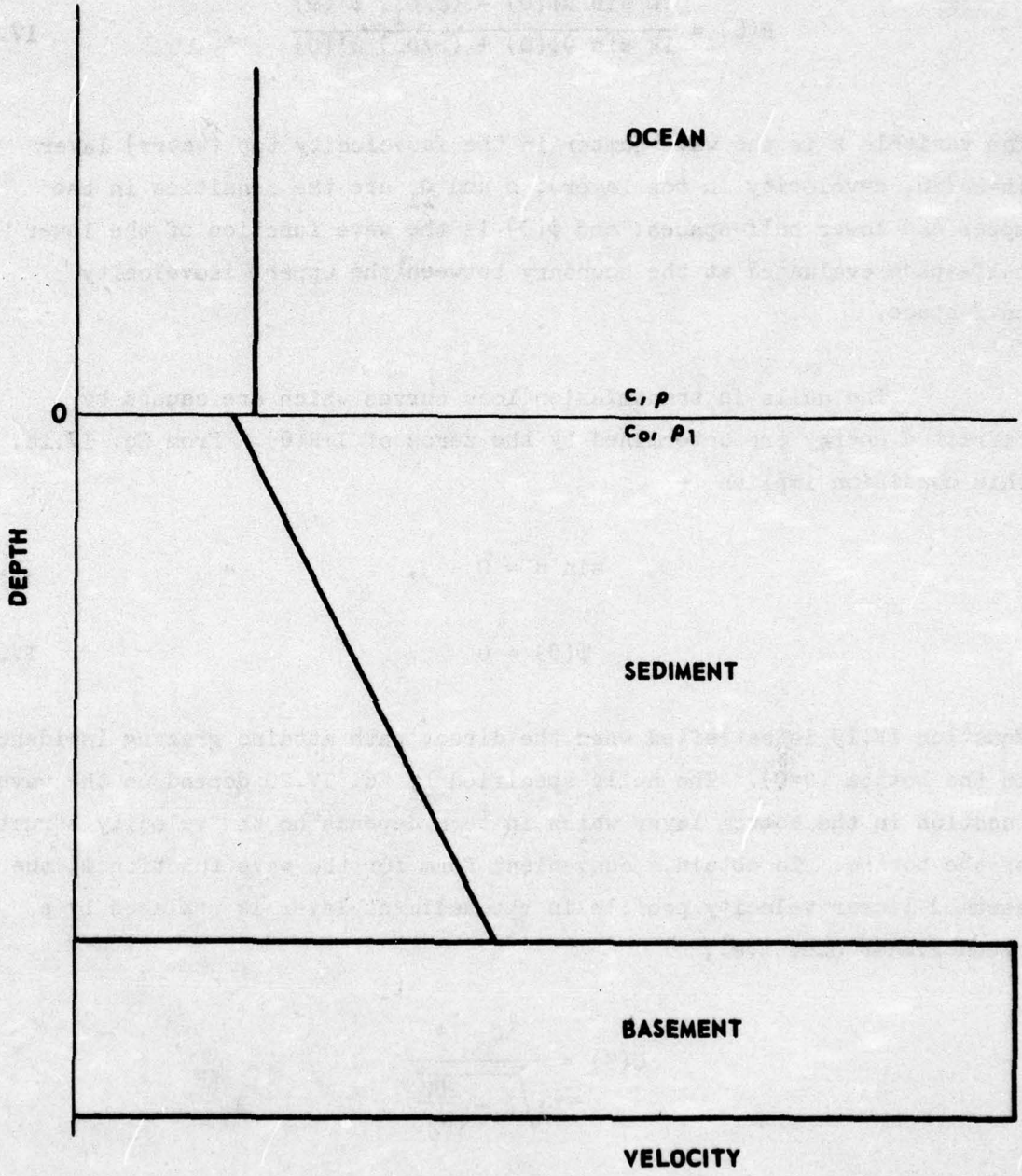

FIGURE IV.3
LAYER CONFIGURATION AND VELOCITY STRUCTURE
(AFTER HANNA)

ARL - UT
AS-76-1213
SRR - DR
11 - 2 - 76

$$R(\theta) = \frac{ik \sin\theta\psi(0) - (\rho/\rho_1)\,\psi'(0)}{ik \sin\theta\psi(0) + (\rho/\rho_1)\,\psi'(0)} \quad . \qquad \text{IV.18}$$

The variable k is the wave number in the isovelocity top (water) layer ($k=2\pi f/c$, c=velocity in top layer), ρ and ρ_1 are the densities in the upper and lower half-spaces, and $\psi(0)$ is the wave function of the lower half-space evaluated at the boundary between the upper, isovelocity half-space.

The nulls in transmission loss curves which are caused by refracted energy are determined by the zeros of $1+R(\theta)$. From Eq. IV.18, this condition implies

$$\sin\theta = 0 \quad , \qquad \text{IV.19}$$

$$\psi(0) = 0 \quad . \qquad \text{IV.20}$$

Equation IV.19 is satisfied when the direct path attains grazing incidence on the bottom ($\theta=0$). The nulls specified by Eq. IV.20 depend on the wave function in the bottom layer which in turn depends on the velocity structure of the bottom. To obtain a convenient form for the wave function ψ, the assumed linear velocity profile in the sediment layer is replaced by a pseudolinear one; i.e.,

$$C(Z) = \frac{C_o}{\sqrt{1 - \frac{2\beta Z}{C_o}}} \quad .$$

This substitution is valid since most of the energy will refract within the depths where the pseudolinear profile is a good approximation to the linear profile.

The use of the pseudolinear profile means that the wave function in the sediment layer is given by the Airy Function; i.e.,

$$\psi(Z) = \mathrm{Ai}\left[\xi(Z)\right]$$

$$\xi(Z) = -\left(\frac{\pi f}{\beta}\right)^{2/3}\left[1 - \left(\frac{C_o}{C}\cos\theta\right)^2 - \frac{2\beta Z}{C_o}\right] \quad .$$

In this case, the condition specified by Eq. IV.20 implies

$$\psi(0) = \mathrm{Ai}\left[\psi(0)\right] = 0 \quad ,$$

or

$$-\left(\frac{\pi f}{\beta}\right)^{2/3}\left[1-\left(\frac{C_o}{C}\cos\theta\right)^2\right] = \alpha_i \quad , \qquad \text{IV.21}$$

where α_i is a zero of the Airy Function.

3. Application of the Method

To see how Hanna's Method is applied, consider the experimental transmission loss curve pictured in Fig. IV.4. The curve was produced from data taken by a bottomed hydrophone over an unconsolidated sediment layer about 1 km thick.

From a knowledge of the source depth and the water profile, those nulls in Fig. IV.4 which arise because of Lloyd's Mirror Effects may be identified. These are the nulls marked A and B in Fig. IV.4. The null marked E is at a range where the direct arrival has grazing incidence and hence may be attributed to Eq. IV.19. The nulls marked C and D must therefore be caused by refracted arrivals. Hanna proposes a method for using the positions of these nulls to evaluate the ratio C_1/C and the gradient at the top of the sediment layer, β.

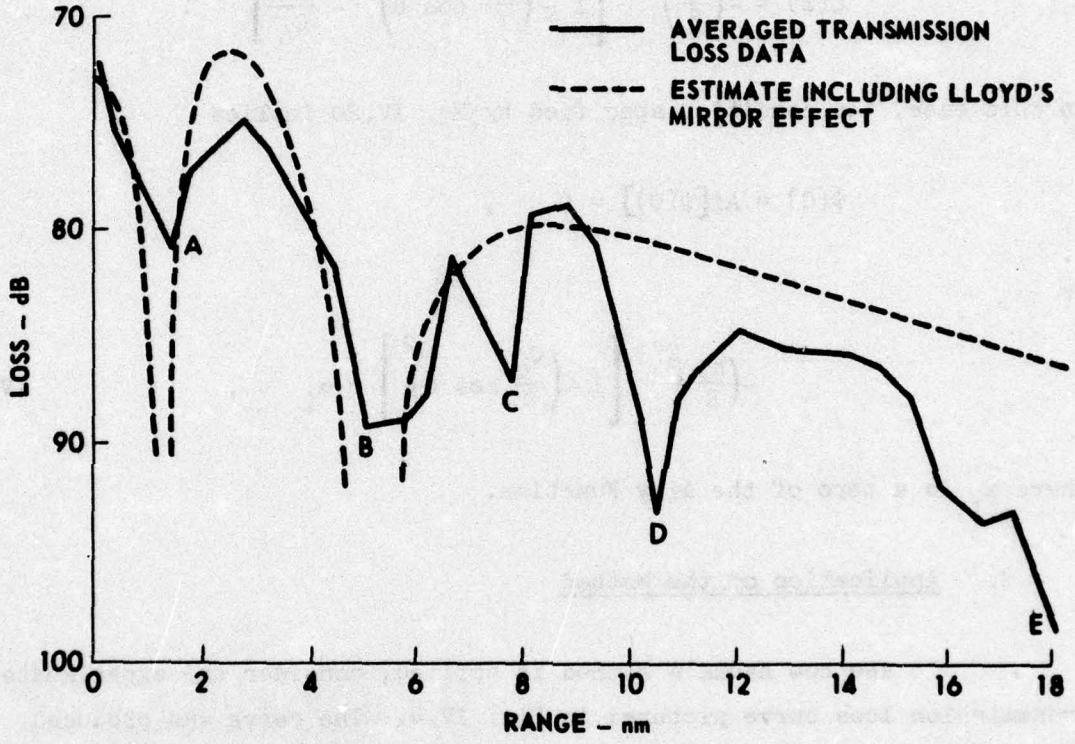

FIGURE IV.4
TRANSMISSION LOSS versus RANGE
(AFTER HANNA)

ARL - UT
AS-76-1214
SRR - DR
11 - 2 - 76

From the range coordinates of the two nulls and a knowledge of the water profile, the grazing angles of the direct arrivals may be determined. With these grazing angles and zeros of the Airy Function, one has two equations like Eq. IV.21 which may be solved simultaneously for C_o/C and β. When Hanna applied this technique to the curve of Fig. IV.4 he obtained the following results which were in good agreement with seismic measurements,

$$C_o/C = 0.98$$

$$\beta = 1.5 \text{ sec}^{-1} \quad .$$

This method can be used to indicate the presence of velocity gradients and to verify or confirm results obtained by other methods. In situations in which propagation loss is the only type of data, this method might well be the only way of obtaining any information about the bottom.

APPENDIX A

DERIVATION OF EXPRESSIONS FOR INTERVAL VELOCITY AND VERTICAL TRANSIT TIME IN A LAYER WITH A CONSTANT GRADIENT

The interval or layer velocity of a layer is defined to be the time averaged velocity through the layer. Although a variety of different expressions for the time averaging are used, the definition used by Clay and Rona[13] will be adopted in this report. Their definition is given in Eq. A.1.

$$C_{int}^{\ 2} = \frac{1}{\Delta T} \int_{o}^{\Delta T} C^2(T)dT \quad . \qquad \text{A.1}$$

The quantity ΔT is the two-way vertical transit time in the layer, and the velocity as a function two-way time, $C(T)$, is referenced to the top of the layer in question.

Next, consider the layer to have a linear sound speed variation, i.e.,

$$C(Z) = C_o + gZ \quad , \qquad \text{A.2}$$

where C_o is the sound speed at the top of the layer, g is the constant gradient, and Z is the vertical coordinate referred to the top of the layer. With Eq. A.2, the vertical two-way time to the depth coordinate Z may be calculated as follows,

$$T = 2 \int_0^Z \frac{dZ}{C(Z)} = \frac{2}{g} \ln\left(1 + \frac{gZ}{C_o}\right) \qquad \text{A.3}$$

If Eq. A.3 is solved for Z, one obtains

$$Z = \frac{C_o}{g}\left(e^{gT/2} - 1\right) . \qquad \text{A.4}$$

If Eq. A.4 is substituted into Eq. A.2, the velocity of sound as a function of two-way time is obtained, i.e.,

$$C(T) = C_o\, e^{gT/2} . \qquad \text{A.5}$$

To calculate the interval velocity, Eq. A.5 is substituted into Eq. A.1 to yield

$$C_{int}^2 = \frac{C_o^2}{\Delta T} \int_0^{\Delta T} e^{gT}\, dT ,$$

$$C_{int}^2 = \frac{C_o^2}{g\Delta T}\left(e^{g\Delta T} - 1\right) . \qquad \text{A.6}$$

Equations A.3 and A.6 are used extensively in the text of this report.

APPENDIX B

DERIVATION OF THE RELATIONSHIP BETWEEN THE RAY PARAMETER AND THE DERIVATIVE OF THE TRAVEL TIME CURVE

A relationship that is frequently used in ray theory is the following one,

$$p = \frac{dT}{dx} \quad . \tag{B.1}$$

The quantity p is the ray parameter of a particular path defined by Snell's Law to be

$$p = \frac{\cos \theta(Z)}{C(Z)} \quad .$$

The derivative in Eq. B.1 is taken along a travel time curve having fixed source and receiver depths. It must be remembered that this is a derivative along a travel time curve, not along a ray path.

Equation B.1 may be obtained by considering two ray paths with infinitesimally differing ray parameters. This configuration is pictured in Fig. B.1. From the geometry of this configuration, in the limit of infinitesimally differing paths, one may write

$$\cos \theta(Z) = \frac{C(Z)dT}{dx}$$

or

$$p = \frac{\cos \theta(Z)}{C(Z)} = \frac{dT}{dx} \quad .$$

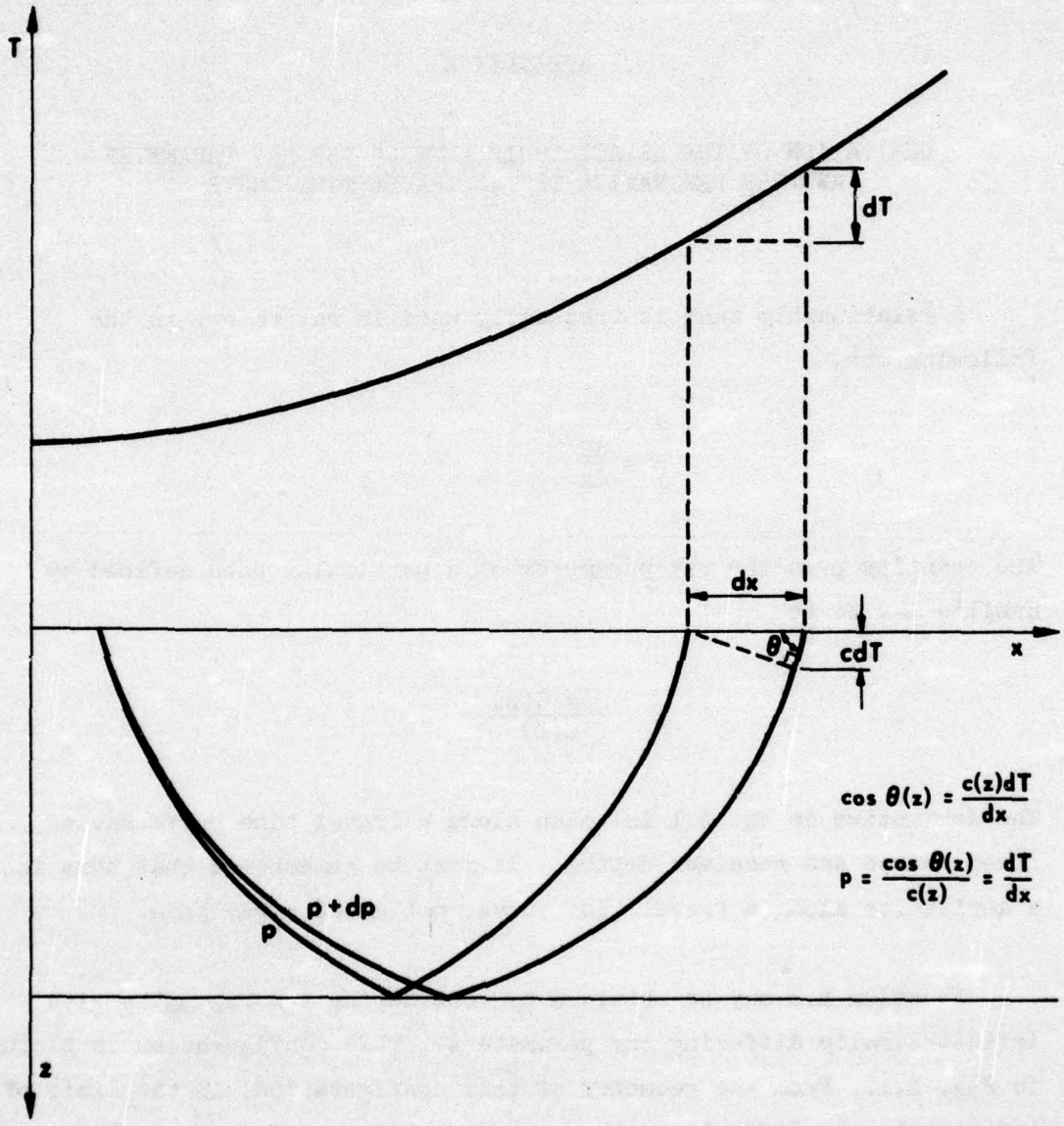

FIGURE B.1
RAY PATH GEOMETRY USED TO SHOW THE RELATION BETWEEN THE RAY PARAMETER AND THE DERIVATIVE OF A TRAVEL TIME CURVE

ARL - UT
AS-76-1215
SRR - DR
11 - 2 - 76

REFERENCES

1. D. J. Shirley and A. L. Anderson, "In situ measurement of marine sediment acoustical properties during coring in deep water," IEEE Transactions on Geoscience Electronics, GE-13(4), pp.163-169, 1975.

2. K. E. Hawker and T. L. Foreman, "A Plane Wave Reflection Coefficient Model Based on Numerical Integration: Formulation, Impelmentation, and Application," Applied Research Laboratories Technical Report No. 76-23 (ARL-TR-76-23), The University of Texas at Austin, Austin, Texas, 1976.

3. C. H. Dix, "Seismic velocities from surface measurements," Geophysics: 20, p. 68-86, 1955.

4. G. L. Maynard, G. H. Sutton, D. M. Hussong, and L. W. Kroenke, "The Seismic Wide Angle Reflection Method in the Study of Ocean Sediment Velocity Structure," from Physics of Sound in Marine Sediments, L. Hampton (ed), Plenum Press, New York, 1974.

5. H. Dürbaum, "Zur Bestimmung von Wellengeschwindigkeiten aus Reflexionsseismischen Messungen," Geophys. Prospecting, 2 pp. 151-167, 1954.

6. G. M. Bryan, "Sonobuoy Measurements in Thin Layers," from Physics of Sound in Marine Sediments, L. Hampton (ed) (Plenum Press, New York, 1974).

7. R. Houtz, J. Ewing, and X. LePichon, "Velocity of deep-sea sediments from sonobuoy data," J. Geophys. Res., 73, 2615-2641, 1968.

8. R. E. Houtz, "Preliminary Study of Global Sediment Sound Velocities from Sonobuoy Data," from Physics of Sound in Marine Sediments, L. Hampton (ed) (Plenum Press, New York, 1974).

9. R. L. Dicus, "Preliminary Investigations of the Ocean Bottom Impulse Response at Low Frequencies," NAVOCEANO Technical Note, TN6130-4-76, 1976.

10. J. S. Hanna, "Short-Range Transmission Loss and the Evidence for Bottom-Refracted Energy," J. Acoust. Soc. Am. 53, 1686-1690 (1973).

11. C. H. Green, "Velocity determinations by means of reflection profiles," Geophysics: 3(4), pp. 295-305, 1938.

12. T. L. Foreman, "Acoustic Ray Models Based on Eigenrays," Applied Research Laboratories Technical Report No. 77-1 (ARL-TR-77-1), The University of Texas at Austin, in preparation.

13. C. S. Clay and P. A. Rona, "Studies of seismic reflections from thin layers on the ocean bottom in the Western North Atlantic," J. Geophys Res., 70, pp. 855-869, 1965.

14. E. L. Hamilton, "Geoacoustic Models of the Sea Floor," from Physics of Sound in Marine Sediments, L. Hampton (ed) (Plenum Press, New York, 1974).

15. L. F. Shampine and R. C. Allen, Numerical Computing: An Introduction (W. B. Saunders Co., Philadelphia, 1973).

21 December 1976

DISTRIBUTION LIST FOR
ARL-TR-76-58
UNDER CONTRACT N00039-76-C-0081
UNCLASSIFIED

Copy No.

1 - 5 Commanding Officer
Naval Electronic Systems Command
Department of the Navy
Washington, DC 20360
Attn: Code 320

6 Commander
Naval Sea Systems Command
Department of the Navy
Washington, DC 20362
Attn: A. P. Franceschetti

Commanding Officer
Naval Ocean Research and Development Activity
National Space Technology Laboratories
Bay St. Louis, MS 39520
7 Attn: CDR E. T. Young (Code 320)
8 Samuel Marshall (Code 340)
9 Herbert Eppert (Code 360)
10 Thomas Pyle (Code 430)
11 Hugo Bezdek (Code 460)
12 Roy Gaul (Code 600)
13 Aubrey L. Anderson (Code 320)

14 Commanding Officer
Office of Naval Research
Arlington, VA 22217
Attn: J. B. Hersey (Code 102-OS)

Commander
Naval Undersea Center
Department of the Navy
San Diego, CA 92132
15 Attn: M. A. Pedersen (Code 307)
16 R. R. Gardner
17 Edwin L. Hamilton
18 Homer P. Bucker (Code 409)
19 H. Morris

AD-A035 697 TEXAS UNIV AT AUSTIN APPLIED RESEARCH LABS F/G 20/1
ANALYTICAL TECHNIQUES FOR DETERMINING SUBBOTTOM VELOCITY PROFIL--ETC(U)
DEC 76 S R RUTHERFORD N00039-76-C-0081
UNCLASSIFIED ARL-TR-76-58 NL

2 OF 2
AD A035697

END
DATE FILMED
3-77

2 OF 2

AD

A035697

Copy No.

Director
Naval Research Laboratory
Department of the Navy
Washington, DC 20375
20 Attn: B. G. Hurdle
21 R. H. Ferris
22 Ronald Dicus (Code 8120)

Naval Oceanographic Office
Department of the Navy
Washington, DC 20373
23 Attn: W. H. Geddes
24 K. V. Mackenzie

25 Commanding Officer
Naval Ocean Research and Development Activity
Liaison Office
Arlington, VA 22217
Attn: R. S. Winokur

Commander
Naval Air Development Center
Department of the Navy
Warminster, PA 18974
26 Attn: C. L. Bartberger
27 P. Haas

Commander
New London Laboratory
Naval Underwater Systems Center
Department of the Navy
New London, CT 06320
28 Attn: F. R. DiNapoli
29 S. R. Santaniello
30 R. L. Deavenport
31 P. Herstein

32 Commanding Officer
Naval Coastal Systems Laboratory
Panama City, FL 32401
Attn: E. G. McLeroy, Jr.

33 Chief of Naval Material
Department of the Navy
Washington, DC 20360
Attn: G. R. Spalding (Code 0345)

Copy No.

Superintendent
Naval Postgraduate School
Monterey, CA 93940
34 Attn: H. Medwin
35 D. Leiper

Woods Hole Oceanographic Institution
Woods Hole, MA 02543
36 Attn: John Ewing
37 Earl E. Hays

38 Morris Schulkin, Consultant
9325 Orchard Brook Drive
Potomac, MD 20854

39 Bolt Beranek and Newman, Inc.
50 Moulton Street
Cambridge, MA 02138
Attn: Preston W. Smith, Jr.

40 Science Applications, Inc.
1651 Old Meadow Road
McLean, VA 22101
Attn: John Hanna

41 Applied Research Laboratory
Pennsylvania State University
P.O. Box 30
State College, PA 16801
Attn: D. C. Stickler

42 Underwater Systems, Inc.
3121 Georgia Avenue
Silver Spring, MD 20910
Attn: Marvin S. Weinstein

Geophysics Laboratory
Marine Science Institute
The University of Texas
700 Strand
Galveston, TX 77550
43 Attn: J. L. Worzel, Director
44 Library

45 TRACOR, Inc.
1601 Research Boulevard
Rockville, MD 20850
Attn: R. J. Urick

Distribution List for ARL-TR-76-58, Contract N00039-76-C-0081 (Cont'd)

Copy No.

46 National Oceanic and Atmospheric Administration
Atlantic Oceanographic and Meteorological Laboratory
15 Rickenbacker Causeway
Miami, FL 33149
Attn: Peter A. Rona

47 Geophysical and Polar Research Center
Department of Geology and Geophysics
The University of Wisconsin
Madison, WI 53700
Attn: C. S. Clay

48 The Catholic University of America
6220 Michigan Avenue, NE
Washington, DC 20017
Attn: H. M. Uberall

Lamont-Doherty Geological Observatory
Palisades, NY 10964
49 Attn: Henry R. Kutschale
50 John E. Nafe
51 R. E. Houtz
52 George M. Bryan

53 Brown University
Providence, RI 02912
Attn: A. O. Williams, Jr.

54 Yale University
Department of Engineering and Applied Science
New Haven, CT 06320
Attn: Franz B. Tuteur

University of Auckland
Physics Department
Auckland, New Zealand
55 Attn: Alick Kibblewhite
56 Kris Tindle

Defence Scientific Establishment
HMNZ Dockyear
Devonport, Auckland
New Zealand
57 Attn: Michael Guthrie
58 R. N. Denham

Distribution List for ARL-TR-76-58, Contract N00039-76-C-0081 (Cont'd)

Copy No.	
59 - 70	Commanding Officer and Director Defense Documentation Center Defense Services Administration Cameron Station, Building 5 5010 Duke Street Alexandria, VA 22314
71	Office of Naval Research Resident Representative Room 582, Federal Building Austin, TX 78701
72 - 73	Environmental Sciences Division, ARL/UT
74	Glen E. Ellis, ARL/UT
75	Karl C. Focke, ARL/UT
76	Terry L. Foreman, ARL/UT
77	Ruth Gonzalez, ARL/UT
78	Loyd D. Hampton, ARL/UT
79	Kenneth E. Hawker, ARL/UT
80	Claude W. Horton, ARL/UT
81	Stephen P. Mitchell, ARL/UT
82	Steve Rutherford, ARL/UT
83	Donald J. Shirley, ARL/UT
84	Jack A. Shooter, ARL/UT
85	Steven L. Watkins, ARL/UT
86	Winifred Williams, ARL/UT
87	Reuben H. Wallace, ARL/UT
88	Library, ARL/UT
89 - 118	Reserve, ARL/UT